



# A test model for fluctuation–dissipation theorems with time-periodic statistics

Boris Gershgorin\*, Andrew J. Majda

Department of Mathematics and Center for Atmosphere and Ocean Science, Courant Institute of Mathematical Sciences, New York University, NY 10012, United States

## ARTICLE INFO

### Article history:

Received 14 September 2009  
 Received in revised form  
 11 March 2010  
 Accepted 26 May 2010  
 Available online 2 June 2010  
 Communicated by J. Bronski

### Keywords:

Fluctuation–dissipation theorem  
 Linear response  
 Exactly solvable model  
 Time-periodic statistics

## ABSTRACT

The recently developed time-periodic fluctuation–dissipation theorem (FDT) provides a very convenient way of addressing the climate change of atmospheric systems with seasonal cycle by utilizing statistics of the present climate. A triad nonlinear stochastic model with exactly solvable first and second order statistics is introduced here as an unambiguous test model for FDT in a time-periodic setting. This model mimics the nonlinear interaction of two Rossby waves forced by baroclinic processes with a zonal jet forced by a polar temperature gradient. Periodic forcing naturally introduces the seasonal cycle into the model. The exactly solvable first and second order statistics are utilized to compute both the ideal mean and variance response to the perturbations in forcing or dissipation and the quasi-Gaussian approximation of FDT (qG-FDT) that uses the mean and the covariance in the equilibrium state. The time-averaged mean and variance qG-FDT response to perturbations of forcing or dissipation is compared with the corresponding ideal response utilizing the triad test model in a number of regimes with various dynamical and statistical properties such as weak or strong non-Gaussianity and resonant or non-resonant forcing. It is shown that even in a strongly non-Gaussian regime, qG-FDT has surprisingly high skill for the mean response to the changes in forcing. On the other hand, the performance of qG-FDT for the variance response to the perturbations of dissipation is good in the near-Gaussian regime and deteriorates in the strongly non-Gaussian regime. The results here on the test model should provide useful guidelines for applying the time-periodic FDT to more complex realistic systems such as atmospheric general circulation models.

© 2010 Elsevier B.V. All rights reserved.

## 1. Introduction

The application of the fluctuation–dissipation theorem (FDT) [1,2] to climate change science has a growing interest among researchers. The classical FDT roughly states that in order to obtain the mean response of the system of identical particles in statistical equilibrium to small external perturbations, it is sufficient to find certain correlation functions of the unperturbed system. Motivated by Kraichnan's generalization of FDT to systems with the Liouville property [3,4], Leith [5] suggested that if the climate system satisfied a suitable fluctuation–dissipation theorem (FDT) then climate response to small external forcing or other parameter changes could be calculated by estimating suitable statistics in the present climate. For the general FDT, see [6–8]. The important practical and conceptual advantages for climate change science when a skillful FDT algorithm can be established is that the linear statistical response operator produced by FDT can be utilized directly for multiple climate change scenarios, multiple changes in forcing, dissipation and other parameters, and inverse

modelling directly [9,10] without the need of running the complex climate model in each individual case, often a computational problem of overwhelming complexity. With these interesting possibilities for FDT, Leith's suggestion inspired a first wave of systematic research [11–16,9,10] for various idealized climate models for the mean response to changes in external forcing. All of this work utilizes the quasi-Gaussian approximation (qG-FDT) suggested by Leith [5,8,17]. Recently, mathematical theory for FDT [8,18–20] has supplied important generalizations and new ways to interpret FDT. These developments have led to improved theoretical understanding of the qG-FDT algorithm, new applications of qG-FDT beyond the mean response with significant skill [10] and new computational algorithms beyond qG-FDT with improved high skill for both the mean and variance of low frequency response which have been tested in a variety of models [21,22,17]. There is also recent mathematical theory for identifying the “most dangerous” perturbations in a given class [8,18]. The above work on algorithms for FDT in climate change science is for forced dissipative large dimensional dynamical systems. Thus, the attractor is a fractal object, typically, but the presence of large dimensional unstable manifolds helps FDT algorithms (see [2,23]) to overcome this lack of smoothness for these high dimensional systems. Furthermore, the short time FDT algorithms developed in [21,22,17] work for systems without any

\* Corresponding author.

E-mail address: [borisg@cims.nyu.edu](mailto:borisg@cims.nyu.edu) (B. Gershgorin).

smoothness on the attractor. However, most of the theories and algorithms developed for FDT assume a stationary climate, which excludes the study of important practical issues of climate change science involving time-periodic statistics such as the diurnal or seasonal cycle.

Very recently generalizations of FDT to time-dependent ensembles were developed by Majda and Wang [18]. As a special case of more general results in their paper, Majda and Wang developed the FDT for time-periodic systems as well as approximate algorithms for climate response with a seasonal cycle. In particular, a quasi-Gaussian algorithm for computing FDT response of a stochastic system with time-periodic invariant measure was proposed in [18]. In a time-periodic setting, the FDT helps to answer such practical questions as how will the time-averaged monthly, seasonal, or yearly mean or variance of certain physical variables change if the external forcing is perturbed. For example, one can be interested in how much the averaged temperature in the month of April will change if the forcing becomes stronger in the month of January.

In this paper, we propose a simple yet very rich triad test model with both periodic deterministic forcing and stochastic forcing as a test bed for time-periodic FDT. This model has already been introduced and used by the authors in applications to filtering problems with multiple time scales [24,25]. The presence of noise makes the attractor smooth and there is a general rigorous justification of FDT in this context [26]. The mathematical formulation of FDT as linear response theory for forced dissipative stochastic dynamical systems is an appropriate setting for these applications since many current improvements in the comprehensive computer models for climate change involve stochastic components [27], while lower dimensional reduced models typically also involve stochastic noise terms [28,20,19].

The key properties of the test model which make it very attractive for testing FDT are

- its exactly solvable structure, i.e., mean, variance and in principle any higher order moments can be computed analytically, therefore, the full ideal response to external perturbations can be found exactly; furthermore, the qG-FDT algorithm can be applied and tested because it requires knowledge of the time-periodic mean and covariance statistics of the unperturbed climate,
- natural time-periodic forcing to study the performance of FDT on the systems with seasonal cycle,
- nonlinear dynamics which provides an opportunity to study both Gaussian and non-Gaussian regimes with the quasi-Gaussian approximation of FDT.

The model is a triad nonlinear stochastic model consisting of one real mode,  $u_1$ , and one complex mode,  $u_2$ , that interacts with  $u_1$  through catalytic nonlinear coupling

$$\frac{du_1}{dt} = -\gamma_1 u_1 + f_1(t) + \sigma_1 \dot{W}_1, \quad (1)$$

$$\frac{du_2}{dt} = (-\gamma_2 + i(\omega_0 + a_0 u_1)) u_2 + f_2(t) + \sigma_2 \dot{W}_2, \quad (2)$$

where  $f_1(t)$  and  $f_2(t)$  are periodic functions of time with the same period  $T_0$ , which represents the annual cycle,  $\gamma_1$ ,  $\gamma_2$ ,  $\sigma_1$ , and  $\sigma_2$  are dissipation and stochastic forcing coefficients that represent the interaction of the triad system with other unresolved modes,  $\omega_0$  is deterministic part of the frequency for the complex mode,  $u_2$ , and  $a_0$  is the coefficient measuring nonlinearity. In [24,25] the authors demonstrated how to use the special structure of the nonlinearity to find analytical formulas for the first and second order statistics of system (1), (2). Here, we use the long time limit of those analytical formulas in order to find statistics in a time-periodic statistical equilibrium. Then, these first and second order statistics can be used for computing

- the “ideal” mean and variance response of the system to the perturbations of external forcing and dissipation,
- the quasi-Gaussian approximation of FDT, which requires the knowledge of mean and covariance statistics of the unperturbed climate.

The test model (1), (2) is motivated by the interaction of a barotropic or baroclinic Rossby wave on a sphere represented by mode the  $u_2$  with Rossby frequency  $\omega_0$  with a strong zonal wind represented by mode  $u_1$ . A special solution to a model similar to system (1), (2) was given in [29] but for the system without stochastic forcing. The forcing  $f_1(t)$  represents the direct forcing of the zonal jet from the polar temperature gradient. On the other hand,  $f_2(t)$  models the forcing of Rossby waves due to baroclinic moist processes or sea surface temperature. Naturally, both of these components of external forcing have a seasonal cycle. The advection of the Rossby wave by the zonal jet is modelled by the nonlinear term with coupling coefficient  $a_0$ . By varying the parameters of the test model we can mimic different scenarios with various ratios of the energies of  $u_1$  and  $u_2$ , various characteristic time scales of these modes compared to the seasonal cycle  $T_0$ , various Rossby wave frequencies when compared with the seasonal cycle (external forcing) frequency, and also various strengths of nonlinearity. By varying the nonlinearity strength,  $a_0$ , we can control the departure of the system statistics from the Gaussian state. As in climate science, we call the period  $[0, T_0]$  a “year” that consists of four equal “seasons” and each season is divided into three equal “months”.

We compute the time-averaged mean response to the changes in forcing and variance response to the changes in dissipation using qG-FDT algorithms. Then, we compare these qG-FDT responses that are given by the linear operators with the corresponding ideal response operators that can be computed using exactly solvable statistics. We choose a number of test cases with various types of system behavior to test the skill of the qG-FDT algorithm for the triad test model (35), (36). We will start by studying near-Gaussian regime where the skill of qG-FDT is very high. Then, we will consider an interesting test case, when the statistics averaged over a certain month or over a full year are near-Gaussian, while the averages over a specific season are strongly non-Gaussian. In a near-Gaussian regime, we expect high skill of the quasi-Gaussian approximation of FDT whereas the strongly non-Gaussian regime is a tough test case for quasi-Gaussian approximation and its skill can deteriorate. Moreover, we will study both resonant and non-resonant situations, when the Rossby wave frequency,  $\omega_0$  is either equal or different from the external forcing frequency. We will find that even though in the resonant case, the system becomes strongly nonlinear and non-Gaussian, the skill of qG-FDT for the mean response to the changes in forcing is surprisingly high and comparable to the skill of qG-FDT in the non-resonant and more Gaussian regimes. On the other hand, the skill of qG-FDT for the variance response to the changes of dissipation deteriorates significantly as the nonlinearity increases.

The rest of the paper is organized as follows. In Section 2, we briefly summarize the general theory for time-dependent FDT. In Section 3, we give a detailed discussion of the triad model (1), (2), its solution and time-periodic equilibrium mean and covariance. There, we also demonstrate how to use the exactly solvable mean and covariance in order to find the ideal mean and variance response to the changes in forcing and dissipation. In Section 4, we compute quasi-Gaussian approximation to the mean and variance response of the triad system (1), (2) to the perturbations of forcing or dissipation. In Section 5, we present the results of our study of the skill of the qG-FDT for the triad system. Finally, in Section 6, we summarize the results of the paper and discuss future work.

## 2. Theory for time-periodic FDT

In this section, we briefly summarize the theory for the time-dependent FDT in a time-periodic statistical steady state. A much more extensive discussion of the subject can be found in [18]. Consider a generic well-posed system of Stochastic Differential Equations (SDE) in the Ito form

$$\frac{du}{dt} = F(u, t) + \sigma(u, t)\dot{W}(t), \quad (3)$$

where  $u \in \mathbb{R}^N$ ,  $F \in \mathbb{R}^N$ ,  $\dot{W}$  is  $M$ -dimensional white noise in time, and  $\sigma$  is an  $N \times M$  matrix. We assume that both  $F(u, t)$  and  $\sigma(u, t)$  are periodic functions of time with the same period  $T_0$ , i.e.,

$$F(u, t + T_0) = F(u, t), \\ \sigma(u, t + T_0) = \sigma(u, t).$$

Eq. (3) models the motion of some physical system. Because of the time-dependent forcing and noise, system (3) does not reach any time-independent statistical equilibrium. However, we can consider time-dependent statistical equilibrium of this system. Of course, even the time-dependent statistical equilibrium may not exist for an arbitrary system (3). However, if the system is dissipative in certain appropriate sense the existence of the statistical equilibrium can be established ([18] and references therein). In particular, we assume that the time-periodic equilibrium is described by the time-periodic pdf,  $p_{\text{eq}}(u, s)$ , with  $p_{\text{eq}}(u, s + T_0) = p_{\text{eq}}(u, s)$  which satisfies the Fokker–Planck equation

$$-\frac{\partial p_{\text{eq}}}{\partial s} - \nabla_u \cdot (p_{\text{eq}}F) + \frac{1}{2} \nabla_u \cdot \nabla_u (\sigma \sigma^T p_{\text{eq}}) = 0. \quad (4)$$

Naturally, two types of averaging arise

- phase average: for any function  $G(u, s)$ , we have

$$\langle G(u, s) \rangle(s) = \int G(u, s) p_{\text{eq}}(u, s) du, \quad (5)$$

- time average: for any periodic function  $f(s)$

$$\langle f(s) \rangle_{T_0} = \frac{1}{T_0} \int_0^{T_0} f(s) ds. \quad (6)$$

The combined average over both phase space and time is defined as

$$\tilde{\langle G(u, s) \rangle} = \langle \langle G(u, s) \rangle \rangle_{T_0}. \quad (7)$$

Note that with such averaging,  $p_{\text{eq}}(u, s)$  becomes a probability measure on the space  $\mathbb{R}^N \times \mathbb{S}^1$

$$\frac{1}{T_0} \int_0^{T_0} \int p_{\text{eq}}(u, s) du ds = 1. \quad (8)$$

Suppose, we are interested in how the mean of some nonlinear functional,  $\hat{A}(u, s)$ , changes when a small perturbation is applied to the forcing  $F(u, t)$ . We consider the perturbations of the general type

$$\delta F(u, t) = a(u, s) \delta f(t), \quad (9)$$

where  $a(u, s)$  is time-periodic vector function,  $f(t)$  is some scalar function of time, and  $\delta$  is a small parameter. Then the time-periodic FDT states [18] that the finite time response of the mean of the nonlinear functional  $\hat{A}(u, s)$  after time  $t$  is given by

$$\delta \tilde{\langle \hat{A}(u, s) \rangle} = \int_0^t R(t - t') \delta f(t') dt', \quad (10)$$

where the response operator is computed via

$$R(t) = \tilde{\langle \hat{A}(u(t + s), t + s) \otimes B_F(u(s), s) \rangle}, \quad (11)$$

and  $u(t)$  is the solution of the phase-shifted dynamical equation

$$\frac{du}{dt} = F(u, t + s) + \sigma(u, t + s)\dot{W}, \quad (12)$$

with the initial condition given as the value of the trajectory at time  $s$

$$u|_{t=0} = u(s). \quad (13)$$

The functional  $B_F(u, s)$  in (11) has the explicit form

$$B_F(u, s) = -\frac{\nabla_u(a(u, s)p_{\text{eq}}(u, s))}{p_{\text{eq}}(u, s)}. \quad (14)$$

The infinite time response of the system to the time-independent perturbation with a constant change in forcing,  $\delta f(t) = \text{const}$ , is given by the linear relationship

$$\delta \tilde{\langle A(u, s) \rangle} = \mathcal{R} \delta f, \quad (15)$$

where the response operator has the form

$$\mathcal{R} = \int_0^\infty R(t) dt. \quad (16)$$

The exact pdf,  $p_{\text{eq}}$ , is often not known for most nonlinear systems; therefore, some approximation of  $p_{\text{eq}}$  is needed [8,18,19]. The simplest approximation is to use the Gaussian pdf,  $p_{\text{eq}}^G(u, s)$ , with the same mean and covariance as in the original system [5,9,10,21,22,17,8,18,19]. This approximation is called the quasi-Gaussian approximation for FDT (qG-FDT). The corresponding functional  $B_F^G$  becomes

$$B_F^G(u, s) = -\frac{\nabla_u(a(u, s)p_{\text{eq}}^G(u, s))}{p_{\text{eq}}^G(u, s)}, \quad (17)$$

and the quasi-Gaussian approximation to the response function (11) is given by

$$R^G(t) = \tilde{\langle \hat{A}(u(t + s), t + s) \otimes B_F^G(u(s), s) \rangle}, \quad (18)$$

while the corresponding infinite time response operator becomes

$$\mathcal{R}^G = \int_0^\infty R^G(t) dt. \quad (19)$$

If the mean and the variance of the time-periodic statistical equilibrium solution of (3) is known the functional in (17) can be computed analytically for a given perturbation (9). In Section 4, we will compute the functional  $B_F^G$  for the test model (1), (2) using exactly solvable first and second order statistics of this model.

Next, we present a few examples of the nonlinear functionals and perturbations. Very general nonlinear functionals have the separable form

$$\hat{A}(u, s) = A(u)\phi(s), \quad (20)$$

where  $\phi(s)$  is periodic with period  $T_0$ . For the response of the mean of  $u$ , we choose

$$[A(u)]_j = u_j, \quad (21)$$

while for the response of the variance, we take

$$[A(u)]_j = (u_j - \langle u_j \rangle)^2. \quad (22)$$

Substituting (20) into (11) and using the change of variables  $s' = s + t$ , we rewrite (11) as

$$R(t) = \frac{1}{T_0} \int_0^{T_0} \phi(t + s) \langle A(u(t + s)) \otimes B_F(u(s), s) \rangle \\ = \frac{1}{T_0} \int_t^{T_0+t} \phi(s') \langle A(u(s')) \otimes B_F(u(s' - t), s' - t) \rangle ds' \\ \stackrel{\text{by periodicity}}{=} \frac{1}{T_0} \int_0^{T_0} \phi(s') \langle A(u(s')) \otimes B_F(u(s' - t), s' - t) \rangle ds'. \quad (23)$$

Suppose we would like to know the response of the time-averaged mean or variance over a part of the period  $[0, T_0]$ , say over  $[t_1, t_2] \subset [0, T_0]$ . Practically, this becomes useful when monthly, seasonal, or annual averages of mean or variance are of interest. Then, the choice of  $\phi(s)$  is the normalized indicator function of the segment  $[t_1, t_2]$

$$\phi(s) = \frac{T_0}{t_2 - t_1} \chi_{t_1, t_2}(s), \tag{24}$$

where

$$\chi_{t_1, t_2}(s) = \begin{cases} 1, & \text{for } s/\text{mod}(T_0) \in [t_1, t_2], \\ 0, & \text{otherwise.} \end{cases} \tag{25}$$

Note that as defined  $\chi_{t_1, t_2}$  is a periodic function of  $s \in \mathbb{R}^1$ . For the special choice of  $\phi(s)$  given in (24), the response function in (23) becomes

$$R(t) = \frac{1}{t_2 - t_1} \int_{t_1}^{t_2} \langle A(u(s)) \otimes B_f(u(s-t), s-t) \rangle ds, \tag{26}$$

and the quasi-Gaussian approximation of  $R(t)$  is

$$R^G(t) = \frac{1}{t_2 - t_1} \int_{t_1}^{t_2} \langle A(u(s)) \otimes B_f^G(u(s-t), s-t) \rangle ds. \tag{27}$$

Next, we discuss two types of perturbations that we are going to study in this paper: perturbations of forcing and perturbations of linear dissipation. Perturbations of forcing are described by (9) with  $a(u, s) = 1$  and the components of the corresponding functional  $B_f$  becomes

$$[B_f]_k = -\frac{\nabla_{u_k} p_{\text{eq}}(u, s)}{p_{\text{eq}}(u, s)}. \tag{28}$$

On the other hand, the perturbations of dissipation are given by  $a(u, s) = -u$  with the functional  $B_d$  given by its components

$$[B_d]_k = \frac{\nabla_{u_k}(u_k p_{\text{eq}}(u, s))}{p_{\text{eq}}(u, s)}. \tag{29}$$

In the quasi-Gaussian approximation, we use the Gaussian pdf,  $p_{\text{eq}}^G$ , instead of the original pdf,  $p_{\text{eq}}$

$$[B_f^G]_k = -\frac{\nabla_{u_k} p_{\text{eq}}^G(u, s)}{p_{\text{eq}}^G(u, s)}, \tag{30}$$

and

$$[B_d^G]_k = \frac{\nabla_{u_k}(u_k p_{\text{eq}}^G(u, s))}{p_{\text{eq}}^G(u, s)}. \tag{31}$$

Now following [18], we discuss practical implementation of (11) or its special case (26) for a given dynamical system (3). In (26) or (27) we use the ergodicity of system (3) and substitute the phase average by the time average over a long time trajectory in a time-periodic equilibrium regime. In order to approximate the probability distribution over the period  $[0, T_0]$ , we discretize this period with  $L$  equal bins centered at points  $s_j$ . Then, the response function (11) can be approximated by

$$R(t) \approx \frac{1}{LT} \sum_{j=1}^L \int_{T^*}^{T^*+T} \hat{A}(u(t+s_j+\tau), t+s_j+\tau) \otimes B_f(u(s_j+\tau), s_j+\tau) d\tau, \tag{32}$$

where  $T \gg 1$ , and  $T^*$  is large enough so that the system (3) has reached time-dependent equilibrium at this time  $T^*$ . Also, we always use  $L = 12$  corresponding to a monthly partition. Below,

we will test the quasi-Gaussian approximation of the time-periodic FDT on the triad model (1), (2).

It is worth remarking here that there are general moment constraints in the time-periodic statistical equilibrium. These constraints allow one to find some higher order statistics recursively knowing the lower order statistics. Then, the response of these higher order statistics to the changes in forcing or dissipation can be found automatically once the response of the lower order statistics is found. Consider a general functional  $G(u, s)$  which is periodic in  $s$  with the period  $T_0$ . Then, we find

$$\begin{aligned} \langle \tilde{\frac{\partial G}{\partial s}} \rangle &= \frac{1}{T_0} \iint \frac{\partial}{\partial s} (G(u, s)) p_{\text{eq}}(s) du ds \\ &= -\frac{1}{T_0} \iint G(u, s) \frac{\partial}{\partial s} p_{\text{eq}}(s) ds du \\ &= \frac{1}{T_0} \iint G(u, s) \left( \nabla(F p_{\text{eq}}) - \frac{1}{2} \nabla \nabla(Q p_{\text{eq}}) \right) du ds \\ &= -\langle F \nabla G \rangle - \frac{1}{2} \langle \sigma \sigma^T \nabla \nabla G \rangle. \end{aligned} \tag{33}$$

To illustrate the simplest moment constraints, consider  $G(u, s) = G_0(u)$  so that (33) becomes the moment constraints

$$\langle \tilde{F \nabla G_0} \rangle + \frac{1}{2} \langle \tilde{\sigma \sigma^T \nabla \nabla G_0} \rangle = 0. \tag{34}$$

Below in Eqs. (56)–(59) of Section 3, we will use constraint (34) to find the annual-averaged third order moment that has an important physical meaning for the system (1), (2)—it represents the energy transfer among the modes.

### 3. Exactly solvable triad model

As we introduced earlier in (1), (2) the model that we use here for testing time-periodic FDT is a stochastic triad nonlinear model with time-periodic deterministic forcing

$$\frac{du_1}{dt} = -\gamma_1 u_1 + f_1(t) + \sigma_1 \dot{W}_1, \tag{35}$$

$$\frac{du_2}{dt} = (-\gamma_2 + i(\omega_0 + a_0 u_1)) u_2 + f_2(t) + \sigma_2 \dot{W}_2, \tag{36}$$

where  $u_1$  is real mode and  $u_2$  is a complex mode. In Eqs. (35) and (36), the parameters  $\gamma_1$  and  $\gamma_2$  represent linear dissipation and  $\sigma_1$  and  $\sigma_2$  represent stochastic forcing. Also,  $\omega_0$  is the deterministic linear frequency of  $u_2$  and  $a_0$  characterizes the strength of nonlinear coupling of  $u_2$  with  $u_1$ . We choose periodic forcings  $f_1(t)$  and  $f_2(t)$  with the same period  $T_0$  which represents seasonal cycle. As we discussed in the introduction, we call the period  $[0, T_0]$  a “year” as in climate science. Naturally, we divide the year into four seasons with each season consisting of three months. System (35), (36) was studied by the authors in [24,25] in a context of filtering. There, it was shown that there exist analytical formulas for the first and second order statistics of  $u_1$  and  $u_2$ . Here, we will use those formulas to compute the exact “ideal” response of the mean and the variance of the system (35), (36) to the perturbations of forcing or dissipation. We are interested in the infinite time response of the system, i.e., we measure the statistics of the system after infinite time has passed since the perturbation was applied. Practically, the relaxation time which is much longer than the system decorrelation time has to pass before the response of the system is measured. Moreover, the time-periodic equilibrium mean and covariance will be used to construct quasi-Gaussian approximation of FDT. The ideal response will be used as a benchmark for the qG-FDT response.

We show how to compute the mean and the variance of  $u_1$  and  $u_2$  by following [24,25]. The solution of Eq. (35) is given by

$$u_1(t) = u_{10}e^{-\gamma_1(t-t_0)} + \int_{t_0}^t f_1(s)e^{-\gamma_1(t-s)} ds + \sigma_1 \int_{t_0}^t e^{-\gamma_1(t-s)} dW_1(s), \quad (37)$$

where  $u_{10}$  is the initial condition at  $t = t_0$ . Now it is easy to find the mean and the variance of  $u_1$ . The mean is given by

$$\langle u_1(t) \rangle = \langle u_{10} \rangle e^{-\gamma_1(t-t_0)} + \int_{t_0}^t f_1(s)e^{-\gamma_1(t-s)} ds. \quad (38)$$

The statistics in the time-periodic equilibrium can be found by sending  $t_0$  to minus infinity, which is equivalent to allowing an infinitely long time to pass after the initial condition is imposed. Then, the time-periodic equilibrium mean of  $u_1$  is given by

$$\langle u_1(t) \rangle_{\text{eq}} = \int_{-\infty}^t f_1(s)e^{-\gamma_1(t-s)} ds. \quad (39)$$

Similarly, the variance of  $u_1$  at time  $t$  with initial condition given at time  $t_0$  becomes

$$\text{Var}(u_1(t)) = \text{Var}(u_{10})e^{-\gamma_1(t-t_0)} + \frac{\sigma_1^2}{2\gamma_1}(1 - e^{-\gamma_1(t-t_0)}). \quad (40)$$

The equilibrium variance becomes

$$\text{Var}_{\text{eq}}(u_1) = \frac{\sigma_1^2}{2\gamma_1}. \quad (41)$$

Note that  $u_1(t)$  is Gaussian and, therefore, it is fully defined by its mean and variance.

Now, we find the mean and the covariance of the second mode,  $u_2$ . The solution of Eq. (36) with initial condition at time  $t_0$  is given by

$$u_2(t) = e^{-\gamma_2(t-t_0)}\psi(t_0, t)u_{20} + \int_{t_0}^t e^{-\gamma_2(t-s)}\psi(s, t)f_2(s) ds + \sigma_2 \int_{t_0}^t e^{-\gamma_2(t-s)}\psi(s, t)dW_2(s), \quad (42)$$

where as in [24,25], we define new functions

$$\psi(s, t) = e^{ij(s,t)}, \quad (43)$$

$$J(s, t) = \int_s^t (\omega_0 + a_0 u_1(s')) ds' = (t-s)\omega_0 + a_0 \int_s^t u_1(s') ds' = J_D(s, t) + J_W(s, t) + b(s, t)u_{10}, \quad (44)$$

where the deterministic part of  $J(s, t)$  is

$$J_D(s, t) = (t-s)\omega_0 + a_0 \int_s^t \int_{t_0}^{s'} f_1(s'')e^{-\gamma_1(s'-s'')} ds'' ds',$$

the noisy part of  $J(s, t)$  is

$$J_W(s, t) = \sigma_1 a_0 \int_s^t ds' \int_{t_0}^{s'} e^{\gamma_1(s'-s'')} dW_1(s''),$$

and the prefactor of  $u_{10}$  is

$$b(s, t) = \frac{a_0}{\gamma_1} (e^{-\gamma_1(s-t_0)} - e^{-\gamma_1(t-t_0)}).$$

The mean of  $u_2$  is given by

$$\langle u_2(t) \rangle = e^{-\gamma_2(t-t_0)} \langle \psi(t_0, t) u_{20} \rangle + \int_{t_0}^t e^{-\gamma_2(t-s)} \langle \psi(s, t) \rangle f_2(s) ds. \quad (45)$$

In the time-periodic equilibrium state the mean of  $u_2$  becomes

$$\langle u_2(t) \rangle_{\text{eq}} = \int_{-\infty}^t e^{-\gamma_2(t-s)} \langle \psi(s, t) \rangle_{\text{eq}} f_2(s) ds. \quad (46)$$

Note that  $J(s, t)$  is Gaussian since it is an integral of the Gaussian variable  $u_1$  plus a deterministic function as can be seen from (44). Therefore,  $\langle \psi(s, t) \rangle_{\text{eq}}$  is by definition a characteristic function of a Gaussian random variable, which has the explicit form

$$\langle \psi(s, t) \rangle_{\text{eq}} = \langle e^{ij(s,t)} \rangle_{\text{eq}} = e^{iJ(s,t)_{\text{eq}} - \frac{1}{2}\text{Var}_{\text{eq}}(J(s,t))}. \quad (47)$$

The mean and the variance of  $J(s, t)$  were computed in [24,25] and here we use those formulas

$$\langle J(s, t) \rangle_{\text{eq}} = (t-s)\omega_0 + a_0 \int_s^t ds' \int_{-\infty}^{s'} f_1(s'')e^{-\gamma_1(s'-s'')} ds'', \quad (48)$$

and

$$\text{Var}_{\text{eq}}(J(s, t)) = \frac{\sigma_1^2 a_0^2}{\gamma_1^3} (e^{-\gamma_1|t-s|} + \gamma_1|t-s| - 1), \quad (49)$$

where again we used  $t_0 \rightarrow -\infty$  as initial time to find time-periodic equilibrium statistics. Similarly, we can find  $\text{Cov}_{\text{eq}}(u_2, u_1)$ ,  $\text{Var}_{\text{eq}}(u_2)$ , and  $\text{Cov}_{\text{eq}}(u_2, u_2^*)$ . We put these computations in the Appendix.

Although expressions (46), (A.7), (A.3) and (A.4) are analytical and explicit, the integrals still have to be computed using numerical quadrature. Exponential decay of the integrands in (46), (A.7), (A.3) and (A.4) suggests that we change variables in order to replace the computation of the integrals over a semi-infinite interval  $(-\infty, t]$  with the computation of the integrals over a finite interval  $[0, 1]$ . We define

$$q \equiv e^{-\gamma_2(t-s)}, \quad (50)$$

which gives

$$s = t + \frac{1}{\gamma_2} \log(q). \quad (51)$$

Then, Eq. (46) becomes

$$\langle u_2(t) \rangle_{\text{eq}} = \frac{1}{\gamma_2} \int_0^1 \langle \psi(s(q), t) \rangle_{\text{eq}} f_2(s(q)) dq. \quad (52)$$

The same approach is used in computing the cross-covariance  $\text{Cov}(u_2, u_1)$  given by (A.7). Similarly, we deal with the double integrals for the second order statistics in (A.3) and (A.4). The change of variables (51) is equivalent to using a non-uniform (logarithmic) mesh in the quadrature for the original variables. Next, we apply the trapezoidal rule. We partition the interval  $[0, 1]$  with points  $q_j$  such that

$$0 = q_0 < q_1 < \dots < q_K = 1, \quad (53)$$

with a small uniform step  $\Delta q = q_{j+1} - q_j$ . Then, the integral of any function  $g(q)$  over the interval  $[0, 1]$  is approximated according to

$$\int_0^1 g(q) dq \approx \frac{\Delta q}{2} (g(q_0) + g(q_K)) + \Delta q \sum_{j=1}^{K-1} g(q_j). \quad (54)$$

Note that in all our examples, the integrand  $g(q)$  vanishes for  $q = 0$  because of the exponential decay to zero of  $\langle \psi(s, t) \rangle$  as  $s \rightarrow -\infty$  (which is equivalent to  $q \rightarrow 0$ ). It is convenient to introduce real variables of the triad system (35) and (36)

$$u = \begin{pmatrix} x_1 \\ x_2 \\ x_3 \end{pmatrix} \equiv \begin{pmatrix} u_1 \\ \text{Re}[u_2] \\ \text{Im}[u_2] \end{pmatrix}. \quad (55)$$

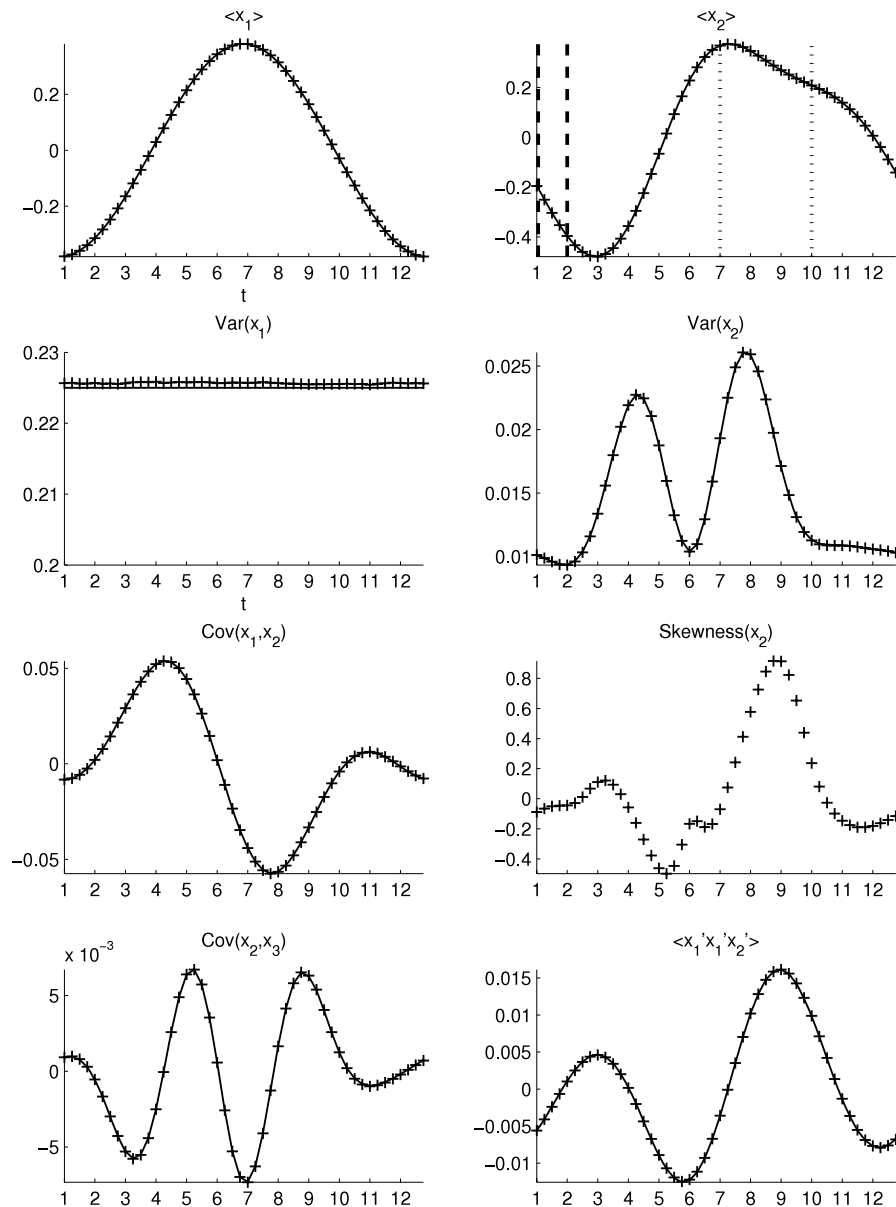


**Fig. 1.** First and second order equilibrium statistics for the triad (55) with the parameters given by the second row in Table 1 (left column and the upper two panels of the right column). Analytically obtained statistics (solid line) are compared with the results of Monte Carlo averaging (pluses). Skewness of  $x_2$  computed through Monte Carlo averaging and the triple correlator  $\langle x_1' x_1' x_2' \rangle$  computed both through Monte Carlo averaging and analytically (lower two panels of the right column). Note that time is measured in months here.

**Table 1**

Description of parameters for different test cases. All four test cases have the same forcing of the first mode,  $f_1(t) = \sin(5\pi/6 \cdot t)$ .

Case	$\gamma_1$	$\gamma_2$	$\sigma_1$	$\sigma_2$	$\omega_0$	$a_0$	$f_2(t)$
1 Near-Gaussian	0.1	0.2	0.1	0.1	$10\pi/6$	1	$0.2e^{i(5\pi/6t+1)}$
2 Non-Gaussian season	0.2	0.4	0.3	0.1	$10\pi/6$	1	$e^{i(5\pi/6t+1)} + 1$
3 Non-resonant forcing	0.1	0.1	0.2	0.2	$\pi$	0.1, 0.2, ..., 0.5	$0.2e^{i(5\pi/6t+1)}$
4 Resonant forcing	0.1	0.1	0.2	0.2	$5\pi/6$	0.05, 0.10, ..., 0.35	$0.2e^{i(5\pi/6t+1)}$

In Fig. 1, we compare the first and second order statistics of the triad (55), computed in this Section analytically with the corresponding results of Monte Carlo ensemble averaging. The conversion formulas for the statistics of the real triad (55) from the statistics of the complex system  $(u_1, u_2)$  are given in the Appendix. Here, we used the parameter set given in the second row of Table 1 (this Table will be discussed below in Section 5). The Monte Carlo averaging was done using a very long trajectory ( $3 \times 10^6$  years) computed via Eq. (37), (42). We used a time step  $h = 10^{-3}$  to approximate the integrals in (46) and in (A.7), (A.3), (A.4). Note

that throughout paper the time is measured in either years or months here, where 1 year is equal to 2.4 time units in terms of the coefficients given in Table 1 and 1 month is 1/12-th of the year.

We note excellent agreement between the analytical formulas and the results of Monte Carlo averaging shown in Fig. 1. Moreover, in Fig. 1, we demonstrate the skewness and flatness of the nonlinear variable  $x_2$  computed using Monte Carlo averaging. We note a large burst of non-Gaussianity in the third season of the annual cycle.

Next, we apply Eq. (34) to compute the annual-averaged third order moment  $\langle \tilde{x}_1 \tilde{x}_2 \tilde{x}_3 \rangle$  that represents the simultaneous energy transfer among the three modes of the system (35), (36) by utilizing combination of the first and second order moments. For any functional  $G_0(u)$ , Eq. (34) becomes

$$\begin{aligned} & \left\langle (-\gamma_1 \tilde{x}_1 + f_1(t)) \frac{\partial G_0}{\partial x_1} \right\rangle \\ & + \left\langle (-\gamma_2 \tilde{x}_2 - \omega_0 \tilde{x}_3 - a_0 \tilde{x}_1 \tilde{x}_3 + \text{Re}[f_2](t)) \frac{\partial G_0}{\partial x_2} \right\rangle \\ & + \left\langle (-\gamma_2 \tilde{x}_3 + \omega_0 \tilde{x}_2 + a_0 \tilde{x}_1 \tilde{x}_2 + \text{Im}[f_2](t)) \frac{\partial G_0}{\partial x_3} \right\rangle \\ & + \frac{1}{2} \left\langle \text{diag}[\sigma_1^2, \sigma_2^2/2, \sigma_2^2/2] \nabla_u \cdot \nabla_u G_0(u, t) \right\rangle = 0, \end{aligned} \quad (56)$$

where  $\text{diag}[\cdot]$  is a diagonal matrix with the given elements. Let us apply this equation to some specific functionals. For  $G_0 = x_3^2$  we find

$$\langle \tilde{x}_1 \tilde{x}_2 \tilde{x}_3 \rangle = \frac{1}{a_0} \left( \gamma_2 \langle \tilde{x}_3^2 \rangle - \omega_0 \langle \tilde{x}_2 \tilde{x}_3 \rangle - \langle \text{Im}[f_2](t) \tilde{x}_3 \rangle - \frac{\sigma_2^2}{4} \right). \quad (57)$$

Similarly, for  $G = x_2^2$  we have

$$\langle \tilde{x}_1 \tilde{x}_2 \tilde{x}_3 \rangle = \frac{1}{a_0} \left( -\gamma_2 \langle \tilde{x}_2^2 \rangle - \omega_0 \langle \tilde{x}_2 \tilde{x}_3 \rangle + \langle \text{Re}[f_2](t) \tilde{x}_2 \rangle + \frac{\sigma_2^2}{4} \right). \quad (58)$$

We add these two expressions to find

$$\begin{aligned} \langle \tilde{x}_1 \tilde{x}_2 \tilde{x}_3 \rangle &= \frac{1}{a_0} \left( -\frac{\gamma_2}{2} (\langle \tilde{x}_3^2 \rangle - \langle \tilde{x}_2^2 \rangle) - \omega_0 \langle \tilde{x}_2 \tilde{x}_3 \rangle \right. \\ & \left. + \frac{1}{2} (\langle \text{Re}[f_2](t) \tilde{x}_2 \rangle - \langle \text{Im}[f_2](t) \tilde{x}_3 \rangle) \right). \end{aligned} \quad (59)$$

Note that, the right hand side of Eq. (59) contains only the first and the second order statistics which can be computed as discussed above. The annual-averaged triple correlator  $\langle \tilde{x}_1 \tilde{x}_2 \tilde{x}_3 \rangle$  is an important physical quantity that measures the energy exchange among all three modes simultaneously, which characterizes the nonlinear wave coupling.

The analytical formulas for the first and second order statistics can be applied to the computation of the ideal response of the triad system to the external perturbation. In particular, in this paper we will be studying the mean response to the changes in forcing and the variance response to the changes in dissipation. The ideal response is the actual linear response to the perturbation and here we know it explicitly for the mean and variance unlike the extensive numerical calculation for this response required for other systems [8,20,9,10]. The ideal response operator computed below will be used as a benchmark for the corresponding qG-FDT response operators that are discussed in Section 4. We start with the ideal mean response to the change in forcing. For simplicity, we drop the subscript “eq” in our notation assuming that all averages are done in the time-periodic statistical equilibrium. We define the real forcing vector

$$f = \begin{pmatrix} f_{x_1} \\ f_{x_2} \\ f_{x_3} \end{pmatrix}. \quad (60)$$

The ideal mean response to the changes in forcing is give by the matrix

$$\mathcal{R}_{M,f}^{\text{id}} = \begin{pmatrix} \frac{\partial \langle \tilde{x}_1 \rangle}{\partial f_{x_1}} & \frac{\partial \langle \tilde{x}_1 \rangle}{\partial f_{x_2}} & \frac{\partial \langle \tilde{x}_1 \rangle}{\partial f_{x_3}} \\ \frac{\partial \langle \tilde{x}_2 \rangle}{\partial f_{x_1}} & \frac{\partial \langle \tilde{x}_2 \rangle}{\partial f_{x_2}} & \frac{\partial \langle \tilde{x}_2 \rangle}{\partial f_{x_3}} \\ \frac{\partial \langle \tilde{x}_3 \rangle}{\partial f_{x_1}} & \frac{\partial \langle \tilde{x}_3 \rangle}{\partial f_{x_2}} & \frac{\partial \langle \tilde{x}_3 \rangle}{\partial f_{x_3}} \end{pmatrix}. \quad (61)$$

Using Eqs. (39) and (46), we find

$$\begin{aligned} \frac{\partial \langle \tilde{x}_1 \rangle}{\partial f_{x_1}} &= \frac{1}{\gamma_1}, \\ \frac{\partial \langle \tilde{x}_1 \rangle}{\partial f_{x_2}} &= 0, \\ \frac{\partial \langle \tilde{x}_1 \rangle}{\partial f_{x_3}} &= 0, \\ \frac{\partial \langle \tilde{x}_2 \rangle}{\partial f_{x_1}} &= -\frac{a_0}{\gamma_1(t_2 - t_1)} \text{Im} \int_{t_1}^{t_2} \int_{-\infty}^t e^{-\gamma_2(t-s)} \langle \psi(s, t) \rangle (t-s) f_2(s) ds dt, \\ \frac{\partial \langle \tilde{x}_3 \rangle}{\partial f_{x_1}} &= \frac{a_0}{\gamma_1(t_2 - t_1)} \text{Re} \int_{t_1}^{t_2} \int_{-\infty}^t e^{-\gamma_2(t-s)} \langle \psi(s, t) \rangle (t-s) f_2(s) ds dt, \\ \frac{\partial \langle \tilde{x}_2 \rangle}{\partial f_{x_2}} &= \frac{\partial \langle \tilde{x}_3 \rangle}{\partial f_{x_3}} = \frac{1}{t_2 - t_1} \text{Re} \int_{t_1}^{t_2} \int_{-\infty}^t e^{-\gamma_2(t-s)} \langle \psi(s, t) \rangle ds dt, \\ \frac{\partial \langle \tilde{x}_2 \rangle}{\partial f_{x_3}} &= -\frac{\partial \langle \tilde{x}_3 \rangle}{\partial f_{x_2}} = -\frac{1}{t_2 - t_1} \text{Im} \int_{t_1}^{t_2} \int_{-\infty}^t e^{-\gamma_2(t-s)} \langle \psi(s, t) \rangle ds dt. \end{aligned}$$

In the Appendix, we show how to find the ideal operator for the variance response to the changes in external forcing,  $\mathcal{R}_{V,f}^{\text{id}}$ , and dissipation,  $\mathcal{R}_{V,d}^{\text{id}}$ .

#### 4. Quasi-Gaussian approximation of FDT for the triad system

In Section 2, we briefly provided a general theory for the time-periodic FDT. There, we obtained the expression for the FDT response operator given by Eq. (11). However, if the time-periodic equilibrium pdf,  $p_{\text{eq}}$ , is not known as happens in most practical approximations, the quasi-Gaussian approximation (18) to the response operator is computed using the Gaussian pdf,  $p_{\text{eq}}^G$  with the same mean and covariance as the original system.

Here, we compute the qG-FDT response operator,  $\mathcal{R}^G$ , for the triad model (55) for the time-averaged mean and variance response to the changes of forcing or dissipation. We will be using different averaging windows that correspond to the first month, the third season, and the full year with formulas as developed in (24)–(27).

For the mean response, the corresponding functional  $A(u)$  in (27) has the form

$$A_M(u) = \begin{pmatrix} x_1 \\ x_2 \\ x_3 \end{pmatrix}, \quad (62)$$

and for the variance response

$$A_V(u) = \begin{pmatrix} (x_1 - \langle x_1 \rangle)^2 \\ (x_2 - \langle x_2 \rangle)^2 \\ (x_3 - \langle x_3 \rangle)^2 \end{pmatrix}. \quad (63)$$

Now, we compute the functional  $B_F^G$  using (30) and (31) for the perturbations of forcing and dissipation, respectively. Note that the Gaussian pdf,  $p_{\text{eq}}^G$ , with the same mean and variance as the solution of the original system (35) and (36) in time-periodic equilibrium is computed analytically using analytical formulas for the first and second order statistics of (35) and (36) obtained in Section 3

$$p^G(u, s) = \frac{1}{\sqrt{(2\pi)^3 |\Sigma|}} \exp\left(-\frac{1}{2}(u - \langle u \rangle)^T \Sigma^{-1} (u - \langle u \rangle)\right), \quad (64)$$

where, the mean,  $\langle u \rangle$ , and the covariance matrix,  $\Sigma$ , of the triad system are computed in the Appendix. For the perturbations of forcing we use (30) and (64) to find

$$[B_f^G(u)]_k = y_k \equiv [\Sigma^{-1}(u - \langle u \rangle)]_k. \quad (65)$$

Then, the quasi-Gaussian approximation (18) of the mean response function to the changes of forcing is given by the matrix with the elements

$$\begin{aligned} [R_{M,f}^G]_{jk}(t) &= \frac{1}{t_2 - t_1} \int_{t_1}^{t_2} \langle A_{M,j}(u(s)) B_{f,k}^G(u(s-t), s-t) \rangle ds \\ &= \frac{1}{t_2 - t_1} \int_{t_1}^{t_2} \langle x_j(s) y_k(s-t) \rangle ds. \end{aligned} \quad (66)$$

Next, we consider perturbations of dissipation by combining (31) and (64)

$$[B_d^G(u)]_k = 1 - x_k [\Sigma^{-1}(u - \langle u \rangle)]_k = 1 - x_k y_k. \quad (67)$$

Then, the quasi-Gaussian approximation (18) of the mean response operator to the changes of dissipation is given by the matrix with the elements

$$[R_{M,d}^G]_{jk}(t) = \frac{1}{t_2 - t_1} \int_{t_1}^{t_2} \langle x_j(s) (1 - x_k(s-t)) y_k(s-t) \rangle ds. \quad (68)$$

Similarly, we find the variance response to changes in forcing

$$[R_{V,f}^G]_{jk}(t) = \frac{1}{t_2 - t_1} \int_{t_1}^{t_2} \langle (x_j(s) - \langle x_j(s) \rangle)^2 y_k(s-t) \rangle ds, \quad (69)$$

and in dissipation

$$\begin{aligned} [R_{V,d}^G]_{jk}(t) \\ = \frac{1}{t_2 - t_1} \int_{t_1}^{t_2} \langle (x_j(s) - \langle x_j(s) \rangle)^2 (1 - x_k(s-t)) y_k(s-t) \rangle ds. \end{aligned} \quad (70)$$

The infinite time response operator,  $\mathcal{R}^G$ , is computed from the response functions,  $R^G(t)$ , via Eq. (19). We note that the quasi-Gaussian response function for the mean to the change of forcing,  $R_{M,f}^G(t)$ , is basically the second order two-time correlation function, for the mean to the changes in dissipation,  $R_{V,f}^G(t)$ , and the variance to the changes in forcing,  $R_{M,d}^G(t)$ , are the third order two-time correlation function, and the variance to the changes in dissipation,  $R_{V,d}^G(t)$ , is the fourth order two-point correlation function. Moreover, the odd order centered statistics of Gaussian random variables vanish [30], and hence, for the near-Gaussian regimes, the mean response to the perturbations of dissipation and variance response to the perturbations of forcing do not deviate from zero significantly. Therefore, in our study we will concentrate on the mean response to the perturbations of forcing and variance response to the perturbations of dissipation.

If we assume that the perturbations of forcing,  $\delta f$ , or perturbations of dissipation,  $\delta \gamma$ , have three independent components,  $\delta f_j$  or  $\delta \gamma_j$ , that correspond to each of the variables  $x_j$  then the corresponding response operators,  $\mathcal{R}$  are  $3 \times 3$  constant coefficient matrices. However, while this assumption of independence of perturbation components is valid for the perturbations of forcing, it is not true

for the perturbations of dissipation because we only have two dissipation parameters,  $\gamma_1$  and  $\gamma_2$ . As we show in the Appendix, the variance response to the changes in dissipation is described by a  $3 \times 2$  constant coefficient matrix. In order to find the corresponding qG-FDT response operator, we equate the perturbations of dissipation for the second and the third components of the triad (55),  $x_2$  and  $x_3$ . This is equivalent to adding the second and the third columns of the qG-FDT response matrix that is obtained under the assumption of independence of all three perturbation components. Then, the qG-FDT variance response to the changes in dissipation is described by a  $3 \times 2$  constant coefficient matrix.

## 5. Skill of the quasi-Gaussian FDT on the test model

In this section, we study the skill of the qG-FDT response for the triad system (35), (36) in comparison with the ideal response. Here, the terminology skill refers to the capability of the quasi-Gaussian FDT approximation to reproduce the exact ideal response reported for example below Eq. (61) for the mean. We have chosen a number of different parameter regimes presented in Table 1 for our tests. As the first test case, we consider a near-Gaussian regime which is the most obvious for testing qG-FDT because the qG-FDT provides an exact ideal response when it is applied to Gaussian systems. As the second test case, we used the regime when the system (35) and (36) has near-Gaussian statistics over the whole year except for the third season, when the pdf deviates from Gaussian significantly. In this regime we expect deteriorating skill for qG-FDT when the time averaging of the statistics is done over this non-Gaussian season. Otherwise, we still anticipate high skill of qG-FDT. In the first two cases, we compared the qG-FDT and ideal mean responses to the changes of forcing. For the third test case, we use a series of simulations for the triad system with a systematically increasing nonlinearity with a forcing that is non-resonant. In this case, we expect qG-FDT to lose skill as the nonlinearity increases and the system becomes more non-Gaussian. Finally, the fourth test case is the same as the third one but with the resonant forcing. Here, the resonant forcing amplifies the statistics of the model and hence the model has large variance and becomes strongly non-Gaussian and, therefore, the qG-FDT is not expected to have much skill as nonlinearity increases. In the third and fourth test cases we compare the mean response to the changes of forcing and the variance response to the changes of dissipation. Below we provide a detailed explanation of the testing procedure presented for the first test case with the near-Gaussian regime. For the remaining test cases we use the same methodology and only discuss the results of our study.

### 5.1. qG-FDT response in the near-Gaussian regime

The first test case represented in Table 1 is characterized by weak damping, weak white noise forcing and weak deterministic forcing of the nonlinear mode,  $u_2$ . This regime is very close to Gaussian and the quasi-Gaussian approximation to FDT is expected to perform well here.

We compare the mean qG-FDT response to the changes in forcing with the corresponding ideal response in this near-Gaussian regime. As discussed in Section 3, we utilize the analytical formulas (39) and (46) of the time-periodic equilibrium mean to find the ideal mean response of the system (35), (36) to the perturbations of forcing. We use three types of time averaging, i.e., monthly average over the first month ( $t_1 = 0$  and  $t_2 = T_0/12$  in Eq. (24)), seasonal average over the third season ( $t_1 = T_0/2$  and  $t_2 = 3T_0/4$  in Eq. (24)), and annual average ( $t_1 = 0$  and  $t_2 = T_0$  in Eq. (24)). We construct the response matrix following the procedure outlined in Section 3. These ideal response operators along with their singular values are given in the upper left quarter of Table 2.

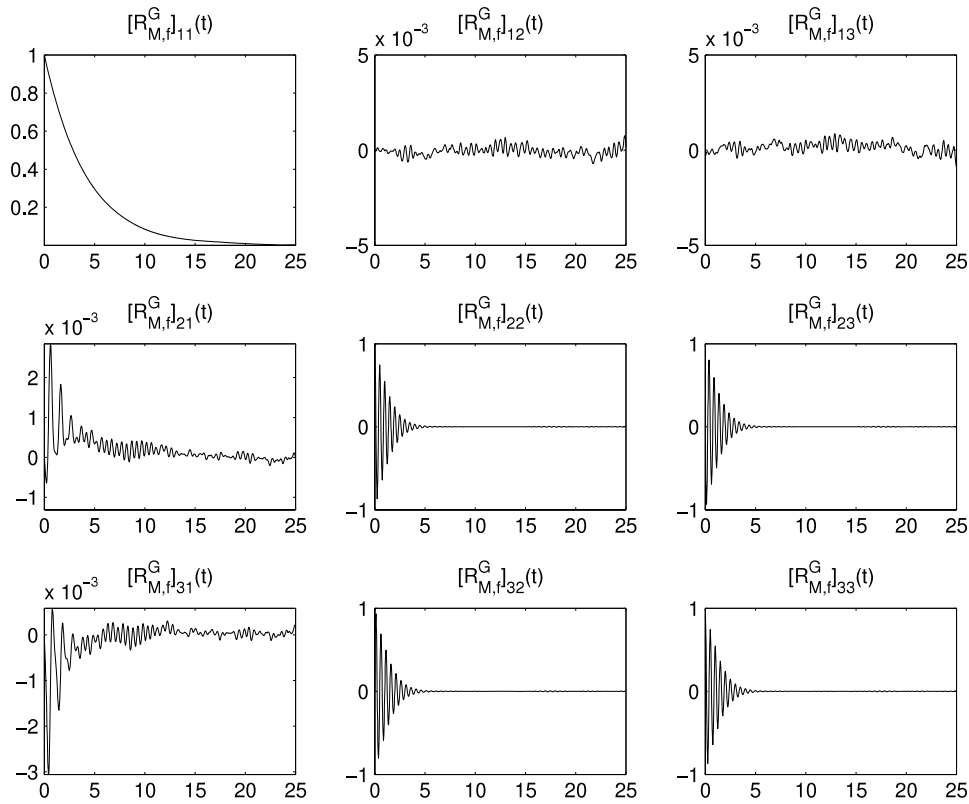


**Fig. 2.** Quasi-Gaussian response function,  $R_{M,f}^G(t)$  (Eq. (66)), for the annual-averaged mean response to the perturbation of forcing for the near-Gaussian regime given in the first row of Table 1. Note that the time is measured in years here.

**Table 2**  
Ideal and qG-FDT operators for the time-averaged mean response to the changes in external forcing and corresponding singular values for test cases 1 and 2 from Table 1.

#	Aver. time	Ideal response				FDT response			
		Operator			Sing. val.	Operator			Sing. val.
1	Month	$\begin{bmatrix} 10.000 & 0.000 & 0.000 \\ -0.908 & 0.015 & -0.212 \\ 0.049 & 0.212 & 0.015 \end{bmatrix}$	$\begin{bmatrix} 10.041 \\ 0.213 \\ 0.212 \end{bmatrix}$	$\begin{bmatrix} 9.837 & -0.003 & 0.003 \\ -0.845 & 0.045 & -0.200 \\ 0.049 & 0.200 & 0.043 \end{bmatrix}$	$\begin{bmatrix} 9.874 \\ 0.205 \\ 0.203 \end{bmatrix}$				
	Season	$\begin{bmatrix} 10.000 & 0.000 & 0.000 \\ -0.660 & 0.012 & -0.184 \\ -0.639 & 0.184 & 0.012 \end{bmatrix}$	$\begin{bmatrix} 10.042 \\ 0.184 \\ 0.183 \end{bmatrix}$	$\begin{bmatrix} 10.075 & -0.004 & 0.004 \\ -0.651 & 0.042 & -0.183 \\ -0.615 & 0.1831 & 0.043 \end{bmatrix}$	$\begin{bmatrix} 10.115 \\ 0.188 \\ 0.186 \end{bmatrix}$				
	Year	$\begin{bmatrix} 10.000 & 0.000 & 0.000 \\ 0.009 & 0.007 & -0.192 \\ -0.010 & 0.192 & 0.007 \end{bmatrix}$	$\begin{bmatrix} 10.000 \\ 0.192 \\ 0.192 \end{bmatrix}$	$\begin{bmatrix} 10.026 & -0.003 & 0.003 \\ 0.010 & 0.033 & -0.190 \\ -0.007 & 0.191 & 0.033 \end{bmatrix}$	$\begin{bmatrix} 10.026 \\ 0.193 \\ 0.193 \end{bmatrix}$				
2	Month	$\begin{bmatrix} 5.000 & 0.000 & 0.000 \\ -0.199 & 0.020 & -0.211 \\ -0.634 & 0.211 & 0.020 \end{bmatrix}$	$\begin{bmatrix} 5.044 \\ 0.212 \\ 0.210 \end{bmatrix}$	$\begin{bmatrix} 4.920 & 0.000 & 0.001 \\ -0.150 & 0.057 & -0.193 \\ -0.654 & 0.243 & 0.030 \end{bmatrix}$	$\begin{bmatrix} 4.966 \\ 0.248 \\ 0.194 \end{bmatrix}$				
	Season	$\begin{bmatrix} 5.000 & 0.000 & 0.000 \\ -0.972 & 0.019 & -0.181 \\ -0.449 & 0.181 & 0.019 \end{bmatrix}$	$\begin{bmatrix} 5.114 \\ \mathbf{0.182} \\ \mathbf{0.178} \end{bmatrix}$	$\begin{bmatrix} 5.028 & -0.001 & -0.003 \\ -0.928 & 0.021 & -0.141 \\ -0.433 & 0.202 & 0.038 \end{bmatrix}$	$\begin{bmatrix} 5.131 \\ \mathbf{0.205} \\ \mathbf{0.140} \end{bmatrix}$				
	Year	$\begin{bmatrix} 5.000 & 0.000 & 0.000 \\ -0.011 & 0.015 & -0.192 \\ -0.222 & 0.192 & 0.015 \end{bmatrix}$	$\begin{bmatrix} 5.005 \\ 0.193 \\ 0.192 \end{bmatrix}$	$\begin{bmatrix} 5.005 & -0.001 & -0.000 \\ -0.013 & 0.038 & -0.196 \\ -0.220 & 0.196 & 0.040 \end{bmatrix}$	$\begin{bmatrix} 5.009 \\ 0.201 \\ 0.199 \end{bmatrix}$				

Next, we test how well the qG-FDT predicts the ideal linear response. The quasi-Gaussian approximation of the response operator,  $\mathcal{R}^G$ , is given by Eq. (19). First, we have to compute the response function,  $R_{M,f}^G(t)$ , which is given by Eq. (18) with the functional  $A$  from (62) and the functional  $B$  from (30). The response function,  $R_{M,f}^G(t)$ , is a two-time correlation function and we use the ergodicity of system (35), (36) to compute  $R_{M,f}^G(t)$  averaging over a long trajectory. We apply the computational algorithm “on the fly” as described in [8] when the correlation function is computed in parallel with to the computation of the trajectory and thus a

very long trajectory can be used in order to achieve a very high precision.

In Fig. 2, we show,  $R_{M,f}^G(t)$ , for each of the components of the operator for the mean to the changes in forcing. Here, we used a long trajectory of the length  $3 \cdot 10^6$  oscillation periods (years). Next, following (19) we integrate,  $R_{M,f}^G(t)$  and obtain the components of the linear response matrix,  $\mathcal{R}_{M,f}^G$ , along with the corresponding singular values given in the upper right quarter of Table 2.

We compare the ideal response matrix with the qG-FDT response matrix to find excellent agreement as we expected for this

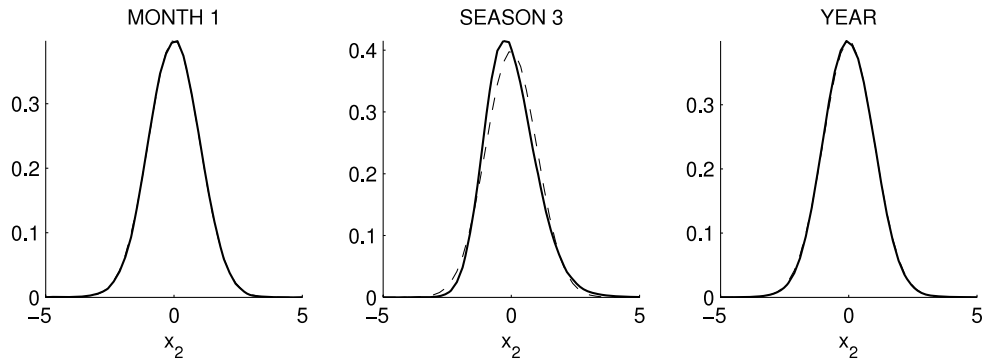


**Fig. 3.** Solid line shows monthly, seasonally, and annually averaged pdfs for the near-Gaussian test case with non-Gaussian season given in the second row of Table 1; the pdfs are rescaled to have mean zeros and variance one. Dashed line shows standard normal distribution  $N(0, 1)$  (on the first and third panels the solid and dashed lines are on top of each other). The pdfs are obtained via Monte Carlo simulation.

near-Gaussian regime. Moreover, we note that annually averaged operators have the best agreement while monthly averaged operators have the worst agreement among the three types of time averaging. This can be explained by the fact that averaging over one certain month requires a much longer trajectory than averaging over the whole year for the same precision. To summarize, we have confirmed that the qG-FDT gives excellent prediction of the mean response operator for the perturbations of forcing for the system in a near-Gaussian regime.

### 5.2. qG-FDT response in the near-Gaussian regime with non-Gaussian season

The second test case represented in Table 1 is characterized by stronger damping of both modes and stronger white noise forcing of the first mode when compared with the first test case from Table 1. Moreover, in the second test case we have stronger forcing  $f_2$  of the nonlinear mode  $u_2$  which creates stronger non-Gaussianity in the statistics of  $u_2$ . In Fig. 1, which we already studied in Section 3, we demonstrate the statistics of the triad (55) for this test case. In Section 3, we used Fig. 1 to confirm that the analytically obtained first and second order statistics coincide with the corresponding results of Monte Carlo averaging. Moreover, the skewness plot in Fig. 1 shows that the system is in the near-Gaussian regime for most of the time except for the burst of non-Gaussianity in the third season (between months 6 and 9). In Fig. 3, we show the pdfs of  $x_2$  for our second test case averaged over the first month, the third season and the whole year. These pdfs were computed in the time-periodic equilibrium and rescaled to have mean zero and variance one. Note that the pdfs here and throughout the rest of the paper are computed using Monte Carlo binning with 80 bins at each time. The pdfs here are used for qualitative demonstration the non-Gaussian properties of the system, on the other hand, the quantitative analysis of the behavior of the qG-FDT algorithm is performed using the exact analytical formulas for the ideal response as discussed in Section 3. We note that the pdf of  $x_2$  averaged over the first month and over the whole year are very close to Gaussian with the corresponding skewness  $-0.07$  and  $0.05$ , respectively. On the other hand, the pdf of  $x_2$  averaged over the third season is significantly non-Gaussian with the skewness  $0.57$ . The source of the non-Gaussianity in the pdf for  $x_2$  can be traced to the triple correlation for anomalies,  $x'_j = x_j - \langle x_j \rangle$  for  $j = 1, 2, 3$ , i.e.,  $\langle x'_1 x'_1 x'_2 \rangle$ ; this triple correlation vanishes identically for a Gaussian random field. In Fig. 1, we plot the skewness of  $x_2$  and the triple correlator,  $\langle x'_1 x'_1 x'_2 \rangle$ , as functions of time over one period. As the reader can see by inspection, these two functionals are highly correlated with pattern correlation  $0.91$ . In the Appendix, we present the analytic formula for  $\langle x'_1 x'_1 x'_2 \rangle$ .

Now, we compare the mean response to the perturbations of forcing, computed using ideal and qG-FDT algorithms as discussed

in Section 5.1. We refer to the lower part of Table 2 now. On the left side, we see the ideal response operator together with the corresponding singular values. Again, we used the averaging over one month (the region, bounded by the dashed vertical lines in the second panel in Fig. 1), over one season (the region, bounded by the dotted vertical lines in the second panel in Fig. 1), and over one year (the whole period). On the right side of the lower part of the Table 2, we show the qG-FDT mean response operators to the changes of forcing along with the corresponding singular values. We note that qG-FDT response operator approximates the ideal response operator quite well when monthly and annual averages are considered. As we mentioned above along these averaging segments, the triad system's statistics are near-Gaussian. However, the qG-FDT operator averaged over the third season is significantly different from the corresponding ideal operator. In particular, we note the difference between the two smallest singular values shown in bold in Table 2. This discrepancy is a consequence of strong non-Gaussianity of the model in the third season.

To conclude the results for the second test case, we have found that for the system with near-Gaussian statistics, the qG-FDT yields a very good approximation of the ideal response operator, while in the non-Gaussian regime, there is a discrepancy between the ideal and qG-FDT mean response to the changes in forcing.

### 5.3. qG-FDT response with the near-resonant forcing

In this and the next sections we study how the skill of the quasi-Gaussian approximation of FDT changes as the system undergoes a transition from a Gaussian to a non-Gaussian regime as the nonlinearity becomes stronger. In this section, we consider non-resonant regimes when the frequency of the forcing  $\omega = 2\pi/T_0$  is different from the frequency  $\omega_0$  of the nonlinear mode  $u_2$ . We gradually increase the strength of the nonlinear coupling which is controlled by the parameter  $a_0$  and study how much the skill of qG-FDT changes. Here, we consider not only the mean response to the changes in forcing given by (19), (66) but also the variance response to the changes in dissipation given by (19), (70). The parameters for the third test case are given in the third row of Table 1.

In Fig. 4, we show the evolution of the pdfs for the non-resonant case for  $a_0 = 0.5$ . The pdfs are shown at the beginning of each of the twelve months. We note that the pdfs here are near-Gaussian by sight. We also note the floating mean position roughly coincides with the position of the peaks of the pdfs. On the other hand, the variance does not change much. In order to quantify non-Gaussianity, in Table 3, we show the dependence of skewness and flatness of the triad model in a time-periodic equilibrium state as the nonlinearity parameter  $a_0$  increases. We used monthly, seasonally, and annually averaged pdfs for computing skewness and flatness. We note that in the regime with non-resonant forcing,

**Table 3**

Variance of  $x_2$  averaged over full year and skewness and flatness of  $x_2$  averaged over first month, third season, and full year for different values of  $a_0$ . Non-resonant forcing test case with the parameters from the third row of Table 1.

$a_0$	Variance	Skewness			Flatness		
		Month 1	Season 3	Year	Month 1	Season 3	Year
0.0	0.100	0.0020	0.0015	−0.0004	3.0084	3.0082	3.0082
0.1	0.101	−0.0015	0.0009	−0.0000	3.0047	3.0041	3.0050
0.2	0.106	−0.0009	0.0068	−0.0003	3.0134	3.0132	3.0106
0.3	0.109	−0.0239	0.0498	0.0001	3.0192	3.0467	3.0494
0.4	0.129	−0.0460	0.1244	0.0003	3.1232	3.1822	3.2842
0.5	0.149	0.0062	0.1755	0.0054	3.5395	3.4259	3.6971

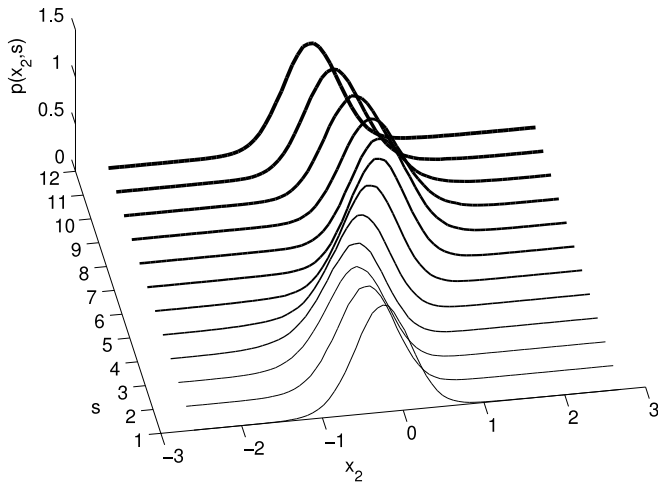


**Fig. 4.** Monthly snapshots of time-dependent equilibrium pdf,  $p(x_2, s)$ , for the non-resonant case given by the third row of Table 1 with  $a_0 = 0.5$ . The pdfs are obtained via Monte Carlo simulation.

the system stays very close to Gaussian even for as high values of nonlinear parameter as  $a_0 = 0.5$ . Therefore, the qG-FDT should have high skill here. However, as we will see in Section 5.4 the situation changes with resonant forcing when the system becomes strongly non-Gaussian even with small values of the nonlinearity parameter  $a_0$ .

To test the skill of the qG-FDT, we followed the procedure outlined in Section 5.1, where we compared the ideal and qG-FDT response operators and their singular values. Here, we only compare the singular values of the corresponding operators. In Table 4, we demonstrate the singular values of the ideal and qG-FDT operators for the time-averaged mean response to the changes in forcing. We note that the corresponding singular values are very close to each other for all values of  $a_0$ . Moreover, the qG-FDT approximations to the response operators for the monthly averaged mean have less skill than the response operators averaged over one season, which in turn have less skill than the operators for the annually averaged mean. As we mentioned in Section 5.1, this is a consequence of the fact that we use the same trajectory to compute the response operators for all three time-averaged statistics, however, the averaging over one month requires more data to achieve the same precision in the correlation function than the average over one season or one year. Next, we consider the variance response to the changes in dissipation. We compute the ideal variance response using Eq. (A.13) from the Appendix. As discussed in Section 3, the operator for the variance response to the changes in dissipation is of the size  $3 \times 2$  and, therefore, it has 2 singular values. When studying the variance response to the changes in dissipation, we should keep in mind that the variance in the non-resonant case is almost independent of time with just a small deviations around its annually averaged value. These annual-averaged values of the variance are given in Table 3 for different values of nonlinearity.

**Table 4**

Singular values of ideal and qG-FDT operators for the time-averaged mean response to the changes in external forcing for the third test case from Table 1 with the non-resonant forcing.

$a_0$	Month		Season		Year	
	Ideal	FDT	Ideal	FDT	Ideal	FDT
0.0	10.000	9.787	10.000	9.960	10.000	9.919
	0.317	0.316	0.317	0.316	0.317	0.319
	0.317	0.315	0.317	0.315	0.317	0.319
0.1	10.025	9.795	10.020	9.960	10.000	9.906
	0.330	0.328	0.308	0.307	0.318	0.320
0.2	0.329	0.328	0.308	0.305	0.318	0.320
	10.110	10.062	10.091	10.212	10.000	10.084
	0.343	0.343	0.299	0.297	0.319	0.321
0.3	0.340	0.339	0.297	0.295	0.319	0.320
	10.285	10.217	10.234	10.340	10.000	10.062
	0.358	0.356	0.289	0.286	0.319	0.321
0.4	0.348	0.346	0.283	0.280	0.319	0.321
	10.579	10.568	10.474	10.639	10.000	10.112
	0.373	0.375	0.277	0.276	0.320	0.325
0.5	0.352	0.361	0.265	0.257	0.320	0.325
	10.957	10.890	10.782	10.912	10.001	10.098
	0.389	0.397	0.264	0.257	0.322	0.330
	0.355	0.377	0.245	0.229	0.322	0.329

We note that the annual-averaged variance grows only a little as  $a_0$  increases. Below, in Table 6 for the resonant forcing regime, we will observe a much more rapid growth of the annual-averaged variance as a function of  $a_0$ . In Table 5, we compare the singular values of the ideal and qG-FDT variance response operators to the changes in dissipation for different values of nonlinearity parameter  $a_0$  for the case of non-resonant forcing. From Table 5, we learn that the skill qG-FDT approximation of the variance response to the changes in dissipation deteriorates as the strength of nonlinearity increases. In particular, we note that the larger singular value is predicted with reasonable accuracy (with ~5% error) only for the nonlinear parameter values up to  $a_0 = 0.3$ . Then, as  $a_0$  increases further, the larger singular value of the qG-FDT operator is significantly larger than that of the ideal operator. This discrepancy for large nonlinearity can be attributed to the fact that the variance response function (70) is the fourth order two-time correlation function, whereas, the quasi-Gaussian approximation is designed to fit the first and the second one-time moments. On the other hand, the smaller singular value is predicted quite well for all values of  $a_0$ .

To summarize, we have tested the qG-FDT approximation of the mean response to the changes in forcing and the variance response to the changes in dissipation on the non-resonant forcing test case. We have seen that the mean response to the changes in forcing is predicted very well for a wide range of nonlinearity parameter  $a_0$ , whereas the variance response to the changes in dissipation slightly deteriorates when the nonlinearity parameter exceeds certain value.

5.4. qG-FDT response with the resonant forcing

Now, we study the test case of resonant forcing with the parameters given in the fourth row of Table 1. In Fig. 5, we demon-

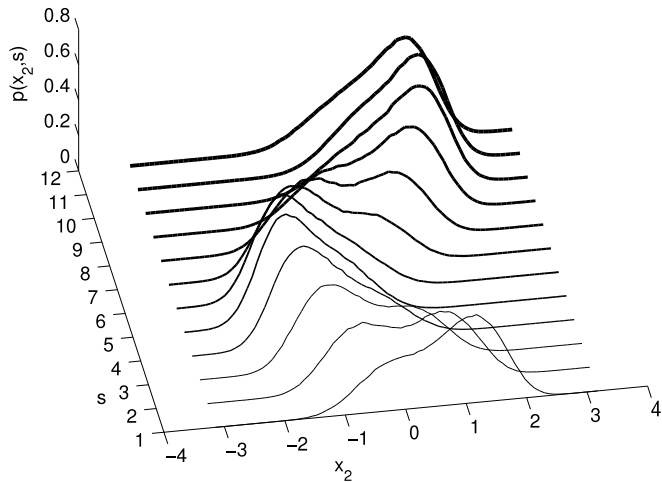


**Fig. 5.** Monthly snapshots of time-dependent equilibrium pdf,  $p(x_2, s)$ , for the resonant case given by the fourth row of Table 1 with  $a_0 = 0.35$ . The pdfs are obtained via Monte Carlo simulation.

strate the monthly snapshots of the evolution of the time-periodic pdf,  $p(x_2, s)$ , of the nonlinear variable  $x_2$  of the triad  $u$  given by (55). Fig. 5 was produced in the strongly nonlinear regime with  $a_0 = 0.35$ . We note that the pdf in Fig. 5 has two peaks during parts of the annual cycle. In Fig. 6, we show the time-averaged pdfs rescaled to have mean zero and variance one for increasing values of  $a_0$  and for three averaging periods over the first month, the third season, and the full year. We compare these pdfs with the standard Gaussian distribution  $N(0, 1)$ . We note that monthly averages are more non-Gaussian than seasonal averages which, in turn, are more non-Gaussian than annual averages. To monitor the departure from Gaussian statistics, we measure corresponding skewness

**Table 5**

Singular values of ideal and qG-FDT operators for the time-averaged variance response to the changes in dissipation for the third test case from Table 1 with the non-resonant forcing.

$a_0$	Month		Season		Year	
	Ideal	FDT	Ideal	FDT	Ideal	FDT
0.0	2.020	1.924	2.020	1.962	2.020	1.952
	1.428	1.410	1.428	1.435	1.428	1.429
0.1	2.020	1.976	2.020	2.008	2.020	2.002
	1.438	1.439	1.438	1.461	1.438	1.457
0.2	2.022	1.969	2.022	2.001	2.022	1.993
	1.475	1.485	1.474	1.510	1.474	1.505
0.3	2.046	2.118	2.045	2.153	2.045	2.144
	1.560	1.549	1.560	1.578	1.559	1.570
0.4	2.252	2.956	2.242	2.986	2.242	2.975
	1.653	1.724	1.650	1.753	1.647	1.742
0.5	2.813	4.958	2.802	4.998	2.799	4.977
	1.667	1.827	1.671	1.870	1.660	1.850

and flatness of  $x_2$  and present them in Table 6. Strong deviations of the system's statistics from Gaussian values show that this is a very tough test case for the qG-FDT. Moreover, in Table 6, we show the annual averages of the variance of  $x_2$  as nonlinearity increases. We note a much faster growth of the annually averaged variance as a function of  $a_0$  than it was in the case with non-resonance forcing (Table 3). The very rapid growth of the variance of  $x_2$  as a function of the nonlinearity strength  $a_0$  is a consequence of resonant forcing.

Next, we study the skill of the qG-FDT response operators. Similar to the non-resonant case discussed in Section 5.3, we first discuss the mean response to the changes in forcing. In Table 7, we show the singular values of the ideal and qG-FDT response operators for three averaging windows (first month, third season, and full year) and for increasing strength of the nonlinearity param-

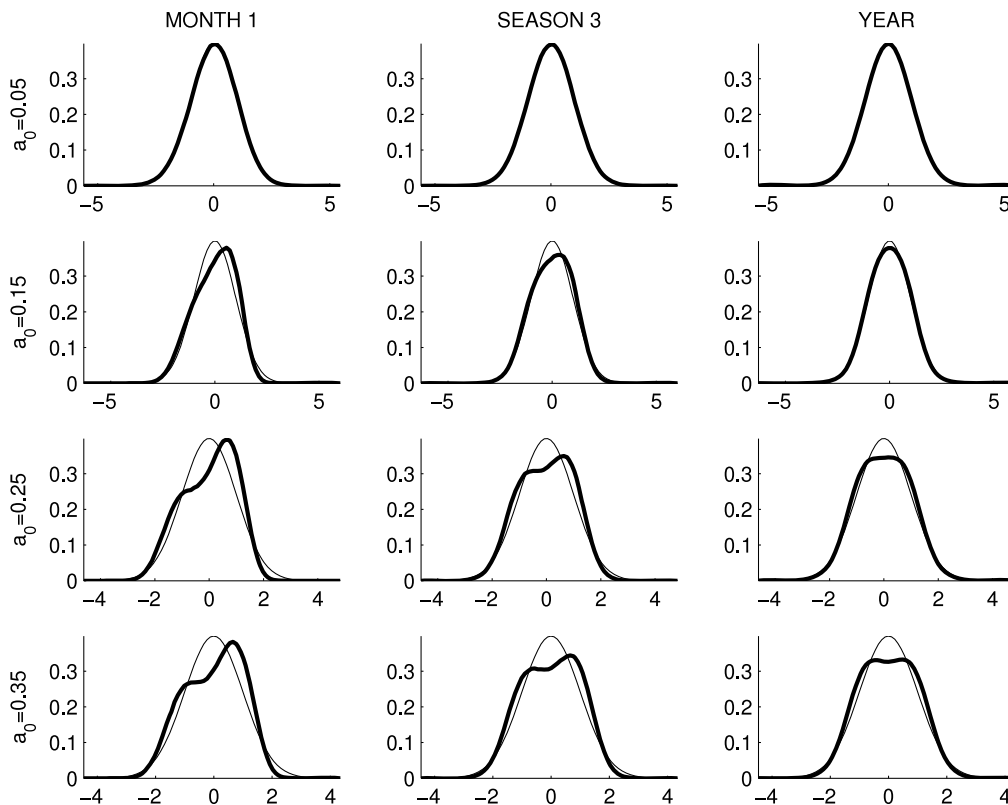


**Fig. 6.** Thick solid line shows the pdfs of  $x_2$  averaged over first month, third season and full year, and rescaled to have mean zero and variance one; thin line shows the standard Gaussian distribution  $N(0, 1)$ . Resonant forcing test case with the parameters from the fourth row of Table 1. The pdfs are obtained via Monte Carlo simulation.

**Table 6**

Variance of  $x_2$  averaged over full year and skewness and flatness of  $x_2$  averaged over first month, third season, and full year for different values of  $a_0$ . Resonant forcing test case with the parameters from the fourth row of Table 1.

$a_0$	Variance	Skewness			Flatness		
		Month 1	Season 3	Year	Month 1	Season 3	Year
0.00	0.10	0.0076	−0.0060	0.0004	3.0168	3.0158	3.0148
0.05	0.14	−0.0901	−0.0189	−0.0000	2.9984	3.0033	3.0256
0.10	0.25	−0.2468	−0.0947	−0.0023	2.7937	2.8481	3.1285
0.15	0.37	−0.3052	−0.1292	−0.0047	2.5346	2.6302	3.0800
0.20	0.47	−0.3145	−0.1309	−0.0061	2.3731	2.4638	2.8673
0.25	0.53	−0.3019	−0.1164	−0.0072	2.3008	2.3626	2.6852
0.30	0.57	−0.2673	−0.1017	−0.0073	2.2434	2.2972	2.5393
0.35	0.59	−0.2310	−0.0953	−0.0069	2.2335	2.2791	2.4535

**Table 7**

Singular values of ideal and qG-FDT operators for the time-averaged mean response to the changes in external forcing for the fourth test case from Table 1 with the resonant forcing.

$a_0$	Month		Season		Year	
	Ideal	FDT	Ideal	FDT	Ideal	FDT
0.00	10.000	9.911	10.000	10.030	10.000	10.030
	0.375	0.348	0.375	0.405	0.375	0.405
	0.375	0.342	0.375	0.401	0.375	0.401
0.05	13.648	13.472	13.090	13.102	10.000	9.986
	0.387	0.365	0.355	0.381	0.377	0.384
	0.284	0.261	0.271	0.296	0.377	0.384
0.10	18.631	18.424	17.434	17.487	10.001	10.074
	0.401	0.380	0.341	0.360	0.380	0.384
	0.215	0.206	0.195	0.206	0.380	0.384
0.15	21.294	20.672	19.772	19.487	10.002	10.067
	0.413	0.395	0.329	0.340	0.381	0.380
	0.194	0.187	0.167	0.179	0.381	0.380
0.20	21.987	20.757	20.368	19.542	10.004	10.061
	0.421	0.417	0.321	0.328	0.382	0.382
	0.192	0.193	0.157	0.170	0.382	0.382
0.25	21.624	19.738	20.027	18.608	10.006	9.969
	0.428	0.435	0.315	0.316	0.382	0.383
	0.198	0.206	0.157	0.170	0.382	0.382
0.30	20.815	18.886	19.294	17.840	10.008	10.105
	0.433	0.447	0.310	0.307	0.382	0.382
	0.208	0.226	0.161	0.175	0.382	0.381
20.35	19.873	17.880	18.448	16.946	10.010	10.177
	0.437	0.460	0.307	0.304	0.383	0.384
	0.220	0.245	0.167	0.181	0.382	0.382

ter  $a_0$ . We note that as the nonlinearity grows, the largest singular value grows significantly for the monthly and seasonal ideal averaged mean responses. Moreover, the other two singular values also depend on the nonlinearity parameter  $a_0$  for the monthly and seasonal ideal averaged mean response operators, one of them decreases and the other one increases as  $a_0$  grows. On the other hand, the singular values of the operator for the annually averaged mean response to the perturbations of forcing are practically independent of  $a_0$ . This phenomenon can be attributed to the fact that annually averaged pdfs of the system are much more Gaussian than the monthly or seasonally averaged pdfs as can be seen from Fig. 6 and Table 6. In Table 7, we compare the ideal and qG-FDT operators for the time-averaged mean response to the changes in forcing and the corresponding singular values. We also show these singular values as function of nonlinearity strength  $a_0$  in Fig. 7 (upper panel). We note surprisingly excellent agreement between the ideal and qG-FDT response operators when compared by the corresponding singular values. Even with the strongest nonlinearity that we considered ( $a_0 = 0.35$ ), the error in predicting the singular values by qG-FDT does not exceed 10%. This numerical experiment shows very high skill of the quasi-Gaussian approximation of FDT for the mean response to the changes in forcing even in a strongly non-Gaussian regime with the two-peaked pdf.

Next, we consider the variance response to the changes in dissipation. We found that the variance stays almost constant over the

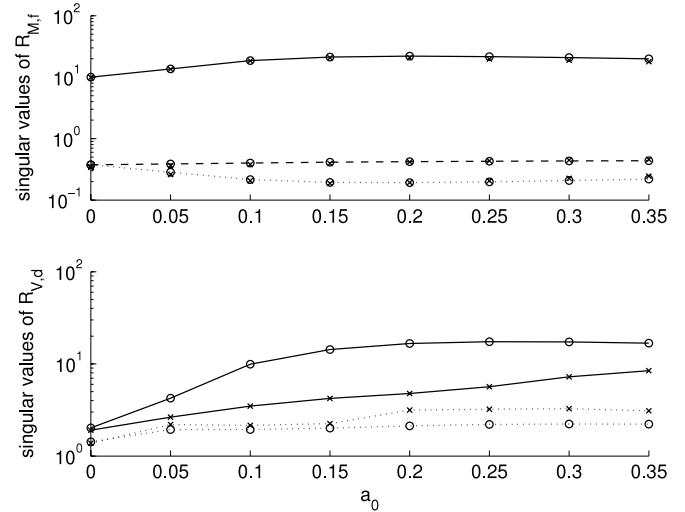


**Fig. 7.** Upper panel: Largest (solid line), medium (dashed line), and smallest (dotted line) singular values of the mean response to the changes in external forcing as functions of  $a_0$ . Singular values of the ideal operator are shown with circles and those of qG-FDT operator are shown with crosses. The response operator is averaged over the first month. Resonant forcing test case with the parameters from the fourth row of Table 1 is shown. The singular values are taken from Table 7. Lower panel: Same as upper panel but for variance response to the changes in dissipation. The larger singular value is shown with solid lines and the smaller singular value is shown with dotted lines. The singular values are taken from Table 8.

whole year period, therefore, the annually averaged values of variance given in Table 6 represent the variance in the each month of the year. We note that the variance increases six times as  $a_0$  grows from  $a_0 = 0$  to  $a_0 = 0.35$ , which is a consequence of the resonant forcing. In Table 8, we compare the ideal and qG-FDT variance response operators to the changes in dissipation and corresponding singular values. We also show these singular values as function of nonlinearity strength  $a_0$  in Fig. 7 (lower panel). We first note that the larger singular value of the ideal variance response to the changes in dissipation grows at an extremely high rate as  $a_0$  grows from  $a_0 = 0$  to  $a_0 = 0.20$ . Then, as  $a_0$  increases further up to  $a_0 = 0.35$ , the larger singular value changes insignificantly. On the other hand, the larger singular value of the qG-FDT variance response to the changes in dissipation has a less rapid but steady growth as  $a_0$  changes from  $a_0 = 0$  to  $a_0 = 0.35$ . The smaller singular value has an opposite trend, i.e., for the ideal operator it grows with a smaller rate than for the qG-FDT operator.

Finally, we consider the monthly response of the variance to changes in external forcing across all months for the resonant forcing case with  $a_0 = 0.35$  (see fourth row in Table 1). This is an extremely difficult test case for the quasi-Gaussian approximation since a purely Gaussian approximation would give zero response [19]. The largest singular value of the ideal response for each month is reported in Fig. 8. There is an extremely strong

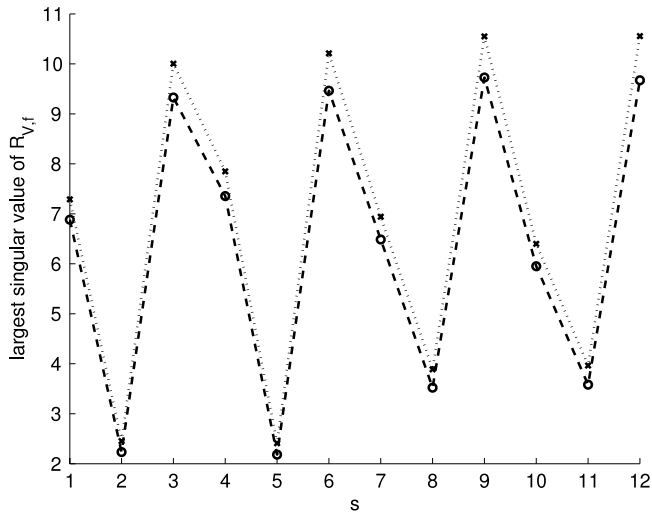


**Fig. 8.** Largest singular value of the variance response to the changes in external forcing for each month. Thick dashed line connects the singular values of the ideal response operator and the dotted line connects the corresponding values of the qG-FDT response operator. Resonant forcing test case with the parameters from the fourth row of Table 1 and  $a_0 = 0.35$ .

variance response at some months and a weaker one elsewhere. This difficult trend is captured very well by the qG-FDT operator (see Fig. 8). The next largest singular value for all months is almost two orders of magnitude smaller and the smallest one is identical zero; both of them are well captured by qG-FDT but not reported here. This provides unambiguous evidence that the qG-FDT algorithm produces the correct correlations among the modes with high skill.

## 6. Conclusions

Time-periodic FDT is tested in this paper on a stochastic nonlinear triad model with periodic forcing and exactly solvable first and second order statistics. The model is designed to mimic the seasonal cycle in the system of two Rossby waves nonlinearly interacting with a zonal jet where the Rossby waves are forced by moist processes and the zonal jet is driven by polar temperature gradient.

We provided a brief introduction to the general time-periodic FDT, in Section 2. Then, in Section 3, we discussed the stochastic triad model and showed how to find analytically first and second (and, in principle, any) order statistics. Next, we explained how these exact statistics are utilized to compute the ideal response of the system for the time-averaged mean and variance to the perturbations of external forcing or dissipation. The ideal response is then used as a benchmark for the response operators obtained via FDT. Then, in Section 4, we showed how to construct quasi-Gaussian approximation to the operators for time-averaged mean and variance response to the changes in forcing and dissipation for the triad model (35), (36). Here, we also need to utilize the exact mean and covariance in order to construct the Gaussian pdf with the same first and second order moments as in the original system. Then, in Section 5, we develop a series of stringent and unambiguous tests for the qG-FDT using the triad model (35), (36), where we compute the skill of the qG-FDT operators for the mean response to the changes in the forcing and for the variance response to the changes in dissipation with the corresponding ideal operators. We have found that in the near-Gaussian regime, qG-FDT has very high skill for the mean response to the changes in the forcing. Moreover, surprisingly this skill stays high even when the system departs from Gaussian regime and even has two-peaked pdf as in Fig. 5. On the other hand, qG-FDT is found to have less

**Table 8**

Singular values of ideal and qG-FDT operators for the time-averaged variance response to the changes in dissipation for the fourth test case from Table 1 with the resonant forcing.

$a_0$	Month		Season		Year	
	Ideal	FDT	Ideal	FDT	Ideal	FDT
0.00	2.020	1.908	2.020	1.934	2.020	1.929
	1.428	1.379	1.428	1.397	1.428	1.389
0.05	4.242	2.646	4.166	2.636	3.931	2.532
	1.942	2.197	1.942	2.230	1.941	2.206
0.10	9.917	3.480	9.726	3.495	9.159	3.407
	1.939	2.155	1.939	2.148	1.936	2.115
0.15	14.338	4.228	14.155	4.287	13.644	4.264
	2.014	2.252	2.001	2.237	1.959	2.098
0.20	16.643	4.780	16.514	4.833	16.171	4.812
	2.126	3.154	2.090	3.044	1.983	2.554
0.25	17.416	5.654	17.331	5.693	17.119	5.546
	2.201	3.225	2.149	3.077	2.001	2.387
0.30	17.317	7.232	17.263	7.213	17.132	7.027
	2.227	3.268	2.169	3.062	2.012	2.388
0.35	16.786	8.437	16.750	8.485	16.668	8.305
	2.220	3.103	2.164	2.959	2.018	2.392

skill in approximating the ideal variance response to the changes in dissipation. We attribute this behavior of qG-FDT to the fact that the variance response to the changes in dissipation is computed using the fourth order two-time correlation function where non-Gaussian effects can be more significant while the mean response to the changes in forcing is computed using the second order two-time correlation function. Moreover, we considered three different averaging times, i.e., averaging over one month, one season, and the whole year. In our test cases, the pdfs averaged over longer time (season or year) were closer to Gaussian state than the pdfs averaged over shorter time (month or season). This led to higher skill of qG-FDT for the statistics averaged over the whole year.

There are a number of directions to proceed with the future work. One can consider a more general type of perturbations of external forcing,  $\delta F = a(u, s)\delta f(t)$ , where  $a(u, s)$  actually depends on  $s$  as in the case of the perturbations of the amplitude of external forcing. Another interesting question to ask is whether we can replace the response function  $R(t)$  given by Eq. (11) with the corresponding correlation only within the averaging time interval. This may seem a simpler approach but it does not have solid theoretical justification. One of the natural applications of the time-periodic FDT is to assess the effects of seasonal cycle on climate change using information theory for finding the most “dangerous” perturbations [8,18]. Also to make an approximation for the FDT with the skill beyond qG-FDT, one can use moment estimators as discussed in [8,29,31]. Finally, the time-periodic FDT developed in [18] and studied here can be applied to realistic General Circulation Models with seasonal cycle to address practical climate change issues. The results developed here for the exactly solvable triad model should provide important guidelines for the behavior of time-periodic FDT for these more complex systems. In particular, the model also allows for exact statistical solutions with time-periodic dissipation and other straightforward more general perturbations.

## Acknowledgements

We thank Fei Hua for the insightful discussion on the variance response to the changes in external forcing. The research of Andrew J. Majda is partially supported by National Science Foundation grant DMS-0456713, the office of Naval Research grant N00014-05-1-0164, and the Defense Advanced Research Projects Agency grant N0014-07-1-0750. Boris Gershgorin is supported as a postdoctoral fellow through the last two agencies.

### Appendix. Second and third order statistics and ideal variance response to the change in forcing and dissipation

We show how to find the second order statistics of  $u_2$  in the time-periodic equilibrium state of the triad system (35), (36). By definition, we have

$$\text{Var}(u_2(t)) = \langle |u_2(t)|^2 \rangle - |\langle u_2(t) \rangle|^2. \quad (\text{A.1})$$

We use Eq. (42) to find

$$\begin{aligned} \langle |u_2(t)|^2 \rangle &= e^{-2\gamma_2(t-t_0)} \langle |u_{20}|^2 \rangle \\ &+ \int_{t_0}^t \int_{t_0}^t e^{-\gamma_2(2t-s-r)} \langle \psi(s, r) \rangle f_2(s) f_2^*(r) ds dr \\ &+ e^{-\gamma_2(t-t_0)} \left( \int_{t_0}^t e^{-\gamma_2(t-s)} \langle u_{20} \psi(t_0, t) \psi^*(s, t) \rangle \right. \\ &\times \left. f_2(s)^* ds + \text{c.c.} \right) + \frac{\sigma_2^2}{2\gamma_2} (1 - e^{-2\gamma_2(t-t_0)}). \end{aligned} \quad (\text{A.2})$$

Next, we consider the time-periodic equilibrium regime by taking the limit  $t_0 \rightarrow -\infty$

$$\begin{aligned} \langle |u_2(t)|^2 \rangle_{\text{eq}} &= \frac{\sigma_2^2}{2\gamma_2} + \int_{-\infty}^t \int_{-\infty}^t e^{-\gamma_2(2t-s-r)} \\ &\times \langle \psi(s, r) \rangle f_2(s) f_2^*(r) ds dr. \end{aligned}$$

Therefore, the equilibrium variance becomes

$$\begin{aligned} \text{Var}_{\text{eq}}(u_2(t)) &= \frac{\sigma_2^2}{2\gamma_2} + \int_{-\infty}^t \int_{-\infty}^t e^{-\gamma_2(2t-s-r)} (\langle \psi(s, r) \rangle \\ &- \langle \psi(s, t) \rangle \langle \psi(r, t) \rangle^*) f_2(s) f_2^*(r) ds dr, \end{aligned} \quad (\text{A.3})$$

where  $\langle \psi(s, t) \rangle$  is given by Eq. (47). Similarly, we find the cross-covariance in time-periodic equilibrium

$$\begin{aligned} \text{Cov}_{\text{eq}}(u_2(t), u_2(t)^*) &= \langle u_2(t)^2 \rangle - \langle u_2(t) \rangle^2 \\ &= \int_{-\infty}^t \int_{-\infty}^t e^{-\gamma_2(2t-s-r)} (\langle \psi(s, t) \psi(r, t) \rangle \\ &- \langle \psi(s, t) \rangle \langle \psi(r, t) \rangle) f_2(s) f_2(r) ds dr, \end{aligned} \quad (\text{A.4})$$

where [24,25]

$$\langle \psi(s, t) \psi(r, t) \rangle = e^{i(J(s,t)+J(r,t))} - \frac{1}{2} (\text{Var}(J(s,t)) + \text{Var}(J(r,t)) + 2\text{Cov}(J(s,t), J(r,t))), \quad (\text{A.5})$$

and  $J(s, t)$  and  $\text{Var}(J(s, t))$  are given by Eqs. (48) and (49), respectively, and

$$\begin{aligned} \text{Cov}(J(s, t), J(r, t)) &= -\frac{\sigma_1^2 a_0^2}{2\gamma_1^3} (1 + 2\gamma_1(\max(s, r) - t) \\ &- e^{-\gamma_1(t-s)} - e^{-\gamma_1(t-r)} + e^{-\gamma_1|s-r|}). \end{aligned} \quad (\text{A.6})$$

Finally, we find the cross-covariance [24,25]

$$\begin{aligned} \text{Cov}_{\text{eq}}(u_2, u_1) &= \frac{i\sigma_1^2 a_0}{2\gamma_1^2} \int_{-\infty}^t f_2(s) e^{-\gamma_2(t-s)} \langle \psi(s, t) \rangle (1 - e^{-\gamma_1(t-s)}) ds. \end{aligned} \quad (\text{A.7})$$

Similarly, we compute the triple correlator  $\langle u'_1 u'_1 u'_2 \rangle_{\text{eq}}$  for  $u'_j = u_j - \langle u_j \rangle$ ,  $j = 1, 2$

$$\begin{aligned} \langle u'_1 u'_1 u'_2 \rangle_{\text{eq}} &= -\frac{\sigma_1^4 a_0^2}{4\gamma_1^4} \int_{-\infty}^t f_2(s) e^{-\gamma_2(t-s)} \langle \psi(s, t) \rangle (1 - e^{-\gamma_1(t-s)})^2 ds. \end{aligned} \quad (\text{A.8})$$

Below, we drop the subscript “eq” for simplicity of notation and assume that all the statistics are computed in the time-periodic equilibrium regime. Here we show how to find the mean and co-

variance of the triad (55) in the time-periodic equilibrium regime. We find that

$$\langle u \rangle_{\text{eq}} = \begin{pmatrix} \langle u_1 \rangle \\ \text{Re}[\langle u_2 \rangle] \\ \text{Im}[\langle u_2 \rangle] \end{pmatrix} = \begin{pmatrix} \langle x_1 \rangle \\ \langle x_2 \rangle \\ \langle x_3 \rangle \end{pmatrix}, \quad (\text{A.9})$$

where  $\langle u_1 \rangle$  is given in Eq. (39) and  $\langle u_2 \rangle$  is given in Eq. (46). The covariance matrix of the triad model (35) and (36) in the time-periodic equilibrium has the form

$$\Sigma = \begin{pmatrix} \text{Var}(x_1) & \text{Cov}(x_1, x_2) & \text{Cov}(x_1, x_3) \\ \text{Cov}(x_1, x_2) & \text{Var}(x_2) & \text{Cov}(x_2, x_3) \\ \text{Cov}(x_1, x_3) & \text{Cov}(x_2, x_3) & \text{Var}(x_3) \end{pmatrix}, \quad (\text{A.10})$$

where

$$\begin{aligned} \text{Var}(x_1) &= \text{Var}(u_1), \\ \text{Var}(x_2) &= \frac{1}{2} (\text{Var}(u_2) + \text{Re}[\text{Cov}(u_2, u_2^*)]), \\ \text{Var}(x_3) &= \frac{1}{2} (\text{Var}(u_2) - \text{Re}[\text{Cov}(u_2, u_2^*)]), \\ \text{Cov}(x_1, x_2) &= \text{Re}[\text{Cov}(u_2, u_1)], \\ \text{Cov}(x_1, x_3) &= \text{Im}[\text{Cov}(u_2, u_1)], \\ \text{Cov}(x_2, x_3) &= \frac{1}{2} \text{Im}[\text{Cov}(u_2, u_2^*)]. \end{aligned} \quad (\text{A.11})$$

Now, we obtain the ideal variance response to the changes in forcing

$$\mathcal{R}_{V,f}^{\text{id}} = \frac{1}{t_2 - t_1} \int_{t_1}^{t_2} \begin{pmatrix} \frac{\partial \text{Var}(x_1)}{\partial f_{x_1}} & \frac{\partial \text{Var}(x_1)}{\partial f_{x_2}} & \frac{\partial \text{Var}(x_1)}{\partial f_{x_3}} \\ \frac{\partial \text{Var}(x_2)}{\partial f_{x_1}} & \frac{\partial \text{Var}(x_2)}{\partial f_{x_2}} & \frac{\partial \text{Var}(x_2)}{\partial f_{x_3}} \\ \frac{\partial \text{Var}(x_3)}{\partial f_{x_1}} & \frac{\partial \text{Var}(x_3)}{\partial f_{x_2}} & \frac{\partial \text{Var}(x_3)}{\partial f_{x_3}} \end{pmatrix} dt, \quad (\text{A.12})$$

where

$$\begin{aligned} \frac{\partial \text{Var}(x_1)}{\partial f_{x_j}} &= 0, \\ \frac{\partial \text{Var}(u_2)}{\partial f_{x_1}} &= \frac{ia_0}{\gamma_1} \int_{-\infty}^t \int_{-\infty}^t e^{-\gamma_2(2t-s-r)} (\langle \psi(s, r) \rangle \\ &- \langle \psi(s, t) \rangle \langle \psi(r, t) \rangle^*) f_2(s) f_2(r)^* (r-s) ds dr \\ \frac{\partial \text{Var}(u_2)}{\partial f_{x_2}} &= \int_{-\infty}^t \int_{-\infty}^t e^{-\gamma_2(2t-s-r)} (\langle \psi(s, r) \rangle \\ &- \langle \psi(s, t) \rangle \langle \psi(r, t) \rangle^*) (f_2(s) + f_2(r)^*) ds dr \\ \frac{\partial \text{Var}(u_2)}{\partial f_{x_3}} &= i \int_{-\infty}^t \int_{-\infty}^t e^{-\gamma_2(2t-s-r)} (\langle \psi(s, r) \rangle \\ &- \langle \psi(s, t) \rangle \langle \psi(r, t) \rangle^*) (f_2(r)^* - f_2(s)) ds dr \\ \frac{\partial \text{Cov}(u_2, u_2^*)}{\partial f_{x_1}} &= \frac{ia_0}{\gamma_1} \int_{-\infty}^t \int_{-\infty}^t e^{-\gamma_2(2t-s-r)} (\langle \psi(s, t) \rangle \langle \psi(r, t) \rangle \\ &- \langle \psi(s, t) \rangle \langle \psi(r, t) \rangle^*) f_2(s) f_2(r) (2t-s-r) ds dr \\ \frac{\partial \text{Cov}(u_2, u_2^*)}{\partial f_{x_2}} &= \int_{-\infty}^t \int_{-\infty}^t e^{-\gamma_2(2t-s-r)} (\langle \psi(s, t) \rangle \langle \psi(r, t) \rangle \\ &- \langle \psi(s, t) \rangle \langle \psi(r, t) \rangle^*) (f_2(s) + f_2(r)) ds dr \\ \frac{\partial \text{Cov}(u_2, u_2^*)}{\partial f_{x_3}} &= i \frac{\partial \text{Cov}(u_2, u_2^*)}{\partial f_{x_2}} \end{aligned}$$

and Eqs. (A.11) were also used.

Now, we obtain the ideal variance response to the changes in dissipation

$$\mathcal{R}_{V,d}^{\text{id}} = \frac{1}{t_2 - t_1} \int_{t_1}^{t_2} \begin{pmatrix} \frac{\partial \text{Var}(x_1)}{\partial \gamma_1} & \frac{\partial \text{Var}(x_1)}{\partial \gamma_2} \\ \frac{\partial \text{Var}(x_2)}{\partial \gamma_1} & \frac{\partial \text{Var}(x_2)}{\partial \gamma_2} \\ \frac{\partial \text{Var}(x_3)}{\partial \gamma_1} & \frac{\partial \text{Var}(x_3)}{\partial \gamma_2} \end{pmatrix} dt, \quad (\text{A.13})$$

where

$$\frac{\partial \text{Var}(x_1)}{\partial \gamma_1} = -\frac{\sigma_1^2}{2\gamma_1^2},$$

$$\frac{\partial \text{Var}(x_1)}{\partial \gamma_2} = 0,$$

$$\frac{\partial \text{Var}(x_2)}{\partial \gamma_1} = \frac{1}{2} \frac{\partial}{\partial \gamma_1} (\text{Var}(u_2) + \text{Re}[\text{Cov}(u_2, u_2^*)]),$$

$$\frac{\partial \text{Var}(x_2)}{\partial \gamma_2} = \frac{1}{2} \frac{\partial}{\partial \gamma_2} (\text{Var}(u_2) + \text{Re}[\text{Cov}(u_2, u_2^*)]),$$

$$\frac{\partial \text{Var}(x_3)}{\partial \gamma_1} = \frac{1}{2} \frac{\partial}{\partial \gamma_1} (\text{Var}(u_2) - \text{Re}[\text{Cov}(u_2, u_2^*)]),$$

$$\frac{\partial \text{Var}(x_3)}{\partial \gamma_2} = \frac{1}{2} \frac{\partial}{\partial \gamma_2} (\text{Var}(u_2) - \text{Re}[\text{Cov}(u_2, u_2^*)]),$$

and the derivatives are computed at the point  $\gamma = (\gamma_1, \gamma_2)^T = 0$ . We use Eqs. (A.3) and (A.4) to find

$$\begin{aligned} \frac{\partial \text{Var}(u_2)}{\partial \gamma_1} &= \int_{-\infty}^t \int_{-\infty}^t e^{-\gamma_2(2t-s-r)} \\ &\times \left[ \frac{\partial \langle \psi(s, r) \rangle}{\partial \gamma_1} - \frac{\partial \langle \psi(s, t) \rangle}{\partial \gamma_1} \langle \psi(r, t) \rangle^* \right. \\ &\left. - \frac{\partial \langle \psi(r, t) \rangle^*}{\partial \gamma_1} \langle \psi(s, t) \rangle \right] f_2(s) f_2^*(r) ds dr \end{aligned} \quad (\text{A.14})$$

and

$$\begin{aligned} \frac{\partial \text{Cov}(u_2, u_2^*)}{\partial \gamma_1} &= \int_{-\infty}^t \int_{-\infty}^t e^{-\gamma_2(2t-s-r)} \\ &\times \left[ \frac{\partial \langle \psi(s, t) \psi(r, t) \rangle}{\partial \gamma_1} - \frac{\partial \langle \psi(s, t) \rangle}{\partial \gamma_1} \langle \psi(r, t) \rangle \right. \\ &\left. - \frac{\partial \langle \psi(r, t) \rangle}{\partial \gamma_1} \langle \psi(s, t) \rangle \right] f_2(s) f_2^*(r) ds dr, \end{aligned} \quad (\text{A.15})$$

where

$$\frac{\partial \langle \psi(s, t) \rangle}{\partial \gamma_1} = \langle \psi(s, t) \rangle \left( i \frac{\partial \langle J(s, t) \rangle}{\partial \gamma_1} - \frac{1}{2} \frac{\partial}{\partial \gamma_1} \text{Var}(J(s, t)) \right),$$

$$\frac{\partial \langle J(s, t) \rangle}{\partial \gamma_1} = -a_0 \int_s^t ds' \int_{-\infty}^{s'} (s' - s'') f_1(s'') e^{-\gamma_1(s' - s'')} ds'',$$

$$\begin{aligned} \frac{\partial}{\partial \gamma_1} \text{Var}(J(s, t)) &= -\frac{3}{\gamma_1} \text{Var}(J(s, t)) \\ &+ \frac{\sigma_1^2 a_0^2}{\gamma_1^3} (t - s) (1 - e^{-\gamma_1(t-s)}), \end{aligned}$$

$$\begin{aligned} \frac{\partial \langle \psi(s, t) \psi(r, t) \rangle}{\partial \gamma_1} &= \langle \psi(s, t) \psi(r, t) \rangle \left( i \frac{\partial \langle J(s, t) \rangle}{\partial \gamma_1} + i \frac{\partial \langle J(r, t) \rangle}{\partial \gamma_1} \right. \\ &\left. - \frac{1}{2} \frac{\partial}{\partial \gamma_1} \text{Var}(J(s, t)) - \frac{1}{2} \frac{\partial}{\partial \gamma_1} \text{Var}(J(r, t)) \right. \\ &\left. + \frac{\partial}{\partial \gamma_1} \text{Cov}(J(s, t), J(r, t)) \right) \end{aligned}$$

$$\begin{aligned} \frac{\partial}{\partial \gamma_1} \text{Cov}(J(s, t), J(r, t)) &= -\frac{3}{\gamma_1} \text{Cov}(J(s, t), J(r, t)) \\ &- \frac{\sigma_1^2 a_0^2}{2\gamma_1^3} (1 + 2(\max(s, r) - t) + (t - s) e^{-\gamma_1(t-s)} \\ &+ (t - r) e^{-\gamma_1(t-r)} - |s - r| e^{-\gamma_1|s-r|}). \end{aligned} \quad (\text{A.16})$$

Next, we compute

$$\begin{aligned} \frac{\partial \text{Var}(u_2)}{\partial \gamma_2} &= -\frac{\sigma_2^2}{2\gamma_2^2} - \int_{-\infty}^t \int_{-\infty}^t (2t - s - r) e^{-\gamma_2(2t-s-r)} (\langle \psi(s, r) \rangle \\ &- \langle \psi(s, t) \rangle \langle \psi(r, t) \rangle^*) f_2(s) f_2^*(r) ds dr, \end{aligned} \quad (\text{A.17})$$

and

$$\begin{aligned} \frac{\partial \text{Cov}(u_2, u_2^*)}{\partial \gamma_2} &= - \int_{-\infty}^t \int_{-\infty}^t (2t - s - r) e^{-\gamma_2(2t-s-r)} (\langle \psi(s, t) \psi(r, t) \rangle \\ &- \langle \psi(s, t) \rangle \langle \psi(r, t) \rangle^*) f_2(s) f_2^*(r) ds dr. \end{aligned} \quad (\text{A.18})$$

## References

- [1] G.S. Agarwal, Fluctuation–dissipation theorems in non-thermal equilibrium and applications, *Z. Phys.* 252 (1972) 25–38.
- [2] U. Marini Bettolo Marconi, A. Puglisi, L. Rondoni, A. Vulpiani, Fluctuation–dissipation: response theory in statistical physics, *Phys. Rep.* 461 (2008) 111–195.
- [3] R.H. Kraichnan, Classical fluctuation–relaxation theorem, *Phys. Rev.* 113 (1959) 1181–1182.
- [4] R.H. Kraichnan, Deviations from fluctuation–relaxation relations, *Physica A* 279 (2000) 30–36.
- [5] C.E. Leith, Climate response and fluctuation dissipation, *J. Atmospheric Sci.* 32 (1975) 2022–2025.
- [6] U. Dekker, F. Haake, Fluctuation–dissipation theorems for classical processes, *Phys. Rev.* 11 (1975) 2043–2056.
- [7] F. Risken, *The Fokker–Planck Equation*, 2nd ed., Springer-Verlag, 1989.
- [8] A.J. Majda, R.V. Abramov, M.J. Grote, *Information Theory and Stochastics for Multiscale Nonlinear Systems*, in: CRM Monogr. Series, American Mathematical Society, 2005.
- [9] A. Gritsun, G. Branstator, Climate response using a three-dimensional operator based on the fluctuation–dissipation theorem, *J. Atmospheric Sci.* 64 (2007) 2558–2575.
- [10] A. Gritsun, G. Branstator, A.J. Majda, Climate response of linear and quadratic functionals using the fluctuation–dissipation theorem, *J. Atmospheric Sci.* 65 (2008) 2824–2841.
- [11] T. Bell, Climate sensitivity from fluctuation dissipation: some simple model tests, *J. Atmospheric Sci.* 37 (1980) 1700–1707.
- [12] G. Carnevale, M. Falcioni, S. Isola, R. Purini, A. Vulpiani, Fluctuation–response in systems with chaotic behavior, *Phys. Fluids A* 3 (1991) 2247–2254.
- [13] G. North, R. Bell, J. Hardin, Fluctuation dissipation in a general circulation model, *Clim. Dyn.* 8 (1993) 259–264.
- [14] A. Gritsun, V. Dymnikov, Barotropic atmosphere response to small external actions. Theory and numerical experiments, *Izv. Atmos. Ocean. Phys.* 35 (1999) 511–525.
- [15] A. Gritsun, Fluctuation–dissipation theorem on attractors of atmospheric models, *Russian J. Numer. Anal. Math. Model.* 16 (2001) 115–133.
- [16] A. Gritsun, G. Branstator, V. Dymnikov, Construction of the linear response operator of an atmospheric general circulation model to small external forcing, *Russian J. Numer. Anal. Math. Model.* 17 (2002) 399–416.
- [17] R. Abramov, A.J. Majda, A new algorithm for low-frequency climate response, *J. Atmospheric Sci.* 66 (2009) 286–309.
- [18] A.J. Majda, X. Wang, Linear response theory for statistical ensembles in complex systems with time-periodic forcing, *Commun. Math. Sci.* 8 (2010) 142–172.
- [19] A.J. Majda, B. Gershgorin, Y. Yuan, Low-frequency climate response and fluctuation–dissipation theorems: theory and practice, *J. Atmospheric Sci.* 67 (4) (2010) 1186–1201.
- [20] A.J. Majda, R. Abramov, B. Gershgorin, High skill in low frequency climate response through fluctuation dissipation theorems despite structural instability, *Proc. Natl. Acad. Sci.* 107 (2010) 581–586.
- [21] R. Abramov, A.J. Majda, Blended response algorithms for linear fluctuation–dissipation for complex nonlinear dynamical systems, *Nonlinearity* 20 (2007) 2793–2821.
- [22] R. Abramov, A.J. Majda, New approximations and tests of linear fluctuation–response for chaotic nonlinear forced–dissipative dynamical systems, *J. Nonlinear Sci.* 18 (2008) 303–341.
- [23] B. Cessac, J.-A. Sepulchre, Linear response, susceptibility and resonances in chaotic toy models, *Physica D* 225 (2007) 13–28.

- [24] B. Gershgorin, A.J. Majda, A nonlinear test model for filtering slow-fast systems, *Commun. Math. Sci.* 6 (2008) 611–649.
- [25] B. Gershgorin, A.J. Majda, Filtering a nonlinear slow-fast system with strong fast forcing, *Commun. Math. Sci.* 8 (2010) 67–92.
- [26] M. Hairer, A.J. Majda, A simple framework to justify linear response theory, *Nonlinearity* 23 (2010) 909–922.
- [27] T. Palmer, P. Williams, *Stochastic Physics and Climate Modelling*, Cambridge University Press, 2010.
- [28] A.J. Majda, C. Franzke, B. Khouider, An applied mathematics perspective on stochastic modelling for climate, *Phil. Trans. R. Soc. A* 366 (2008) 2429–2455.
- [29] A.J. Majda, X. Wang, *Nonlinear Dynamics and Statistical Theories for Basic Geophysical Flows*, Cambridge University Press, 2006.
- [30] C.W. Gardiner, *Handbook of Stochastic Methods: For Physics, Chemistry and the Natural Sciences*, 3rd ed., Springer-Verlag, New York, 2004.
- [31] R. Abramov, Short-time linear response with reduced-rank tangent map, *Chin. Ann. Math. Ser. B* 30 (2009) 447–462.